

# 5<sup>th</sup> MEETING of THE CZECH TECTONIC STUDIES GROUP

BUBLAVA - KRUŠNÉ HORY, April 12 - 15, 2000

## EXCURSION GUIDE

TO THE MOST BASIN AND KRUŠNÉ HORY MTS.

*published in Prague, April 1999*

*by the Institute of Geology, Academy of Sciences of the Czech Republic*

## DAY 1

# Sedimentation and Syndimentary Deformation in a Rift-margin, Lacustrine Delta System: the Bílina Delta (Miocene), Most Basin

David ULIČNÝ<sup>1</sup>, Michal RAJCHL<sup>1</sup>, Karel MACH<sup>2</sup> and Zdeněk DVOŘÁK<sup>2</sup>

<sup>1</sup> Department of Geology, Charles University, Albertov 6, 128 43 Praha 2, Czech Republic

<sup>2</sup> Severočeské doly, a.s., Doly Bílina, 5 května 213, 4180 29 Bílina, Czech Republic

### Introduction

This field trip focuses on spectacular exposures of a lacustrine delta system of the Miocene Bílina Delta (Hurník 1959, 1978; Rajchl and Uličný 1999; Dvořák and Mach 2000) in the Bílina Mine, owned by the Severočeské doly, a.s. Because of ongoing mining activity and constantly changing exposure in the open-cast coal mine, it is not possible to include fixed „field stops“ as in a traditional field guide. Instead, this field guide introduces the main sedimentological phenomena of the Bílina Delta system, illustrates their typical examples, and provides a geological background to the features observed during the field trip. Some of the features figured in this guide have been quarried away during the last 1–2 years, but the field trip participants will be able to observe many similar features that are not yet exposed at the time of writing this guide.

This guide is based on completed as well as ongoing research by the authors, who wish to thank the Severočeské doly, a.s., for financial support and logistical cooperation. Part of the research by M. Rajchl and D. Uličný was also supported by a grant from the Czech Academy of Sciences, GA AV ČR Grant No. A3012705.

### Regional Background: the most basin as a part of the Ohře (Eger) graben system

The Ohře (Eger) Graben is a major tectonosedimentary feature of Central Europe, characterized by a system of Cenozoic sedimentary basins and intense intraplate alkaline volcanism (Fig. 1; Kopecký 1978; Sengör 1995; Wilson 1993; Cajz et al. 1999; Adamovič and Coubal 1999). Although the Ohře Graben has long been recognized as a part of the Central European Rift System (Ziegler 1990), its structural evolution, and, especially, its relation to sedimentary basin formation, remain poorly understood.

In the present-day geological picture, the Most Basin is one of four major sedimentary basins preserved in the Ohře Graben and separated from one another by volcanic domains and fault systems which cross-cut the Ohře Graben axis at high angles (Fig. 1). It is important to note that the prominent, NE-trending fault systems, which confine the Most and Sokolov (and, partly, also Zittau) basins as essentially erosional relicts in the present-day topography, are relatively young compared to the basin fill (cf. Adamovič and Coubal 1999). Current research on the geometries of individual depocentres and depositional patterns within the basins of the Ohře Graben (Rajchl and Uličný 2000; Špičáková et al. 2000) shows that during the main phase of rift sedimentation, the whole Ohře Graben was dominated by oblique extension, driven by a palaeostress field characterized by NNE-oriented horizontal extension (i.e., at angles approximately between 45 and 60° to the rift axis; cf. Fig. 1 and 2). This is in partial agreement with the results of Adamovič and

Coubal (1999) who infer a N–S extension dominating the emplacement of volcanics between c. 32–24 Ma in parts of the rift system. However, the tentative reconstruction of the oblique rifting geometry (Fig. 1) suggests that the NNE–SSW-oriented extensional regime could have persisted for a longer time and was probably more regionally consistent than expected by the above authors.

The rift axis (or, axis of extension; Fig. 1) probably corresponds, at a deeper crustal level, to a major crustal inhomogeneity, in the central and northern parts of the rift located at the major gravity field gradient, interpreted by most authors as the boundary between the Saxothuringian and the Teplá-Barrandian terranes (commonly associated with the hypothetical Lito-měřice Deep Fault – e.g., Blížkovský et al. 1988). Among the shallow structures occurring in the Ohře Graben, the Střezov Fault, coinciding with the marginal fault of the Permo-Carboniferous Žatec Basin, is probably the only surficial manifestation of this deep crustal anisotropy. However, it should be noted that the NE and SW ends of the Ohře Graben axis do not exactly follow the bending trace of the gravity gradient, and rather suggest propagation of the zone of extensional faulting beyond the control of the deep crustal inhomogeneity.

The Most Basin represents the central part of the Ohře Graben, where the rift axis runs highly oblique to the presumed extension vector. Construction of isopach maps of the basin fill and revision of geological maps and cross-sections from the mining fields of the Most Basin, together with a digital terrain model study (Rajchl and Uličný 2000) shows that during the deposition of clastic sediments coals and volcanoclastics of the basin fill, the basin geometry was controlled by approximately E–W (ENE–WSW)-striking normal faults, along which individual depocentres of the Most Basin formed. In plan view, the short fault segments are arranged in an en-echelon pattern and were probably divided by relay ramps (cf. Peacock and Sanderson 1994; McClay and White 1995). The same en-echelon arrangement is observed in the positions of depocentres, divided by palaeohighs which coincide with locations of transverse, NW-striking, basement fault zones. Research is under way to clarify whether the palaeohighs separating the depocentres were „soft“ accommodation zones or the reactivation of basement fractures caused „hard“ separation between arrays of opposite-dipping extensional faults. The fault pattern and depocentre geometries of the Most Basin can be compared with oblique-rift settings described e.g. by Morley et al. (1992) and, notably, with the analogue models of oblique rifts by McClay and White (1995) or Tron and Brun (1991).

This E–W fault pattern is largely subdued in present-day topography, due to a strong overprint by the NE-trending fault systems. However, the en-echelon syndepositional normal faults which bounded the depocentres of the Oligo-Miocene rift ba-

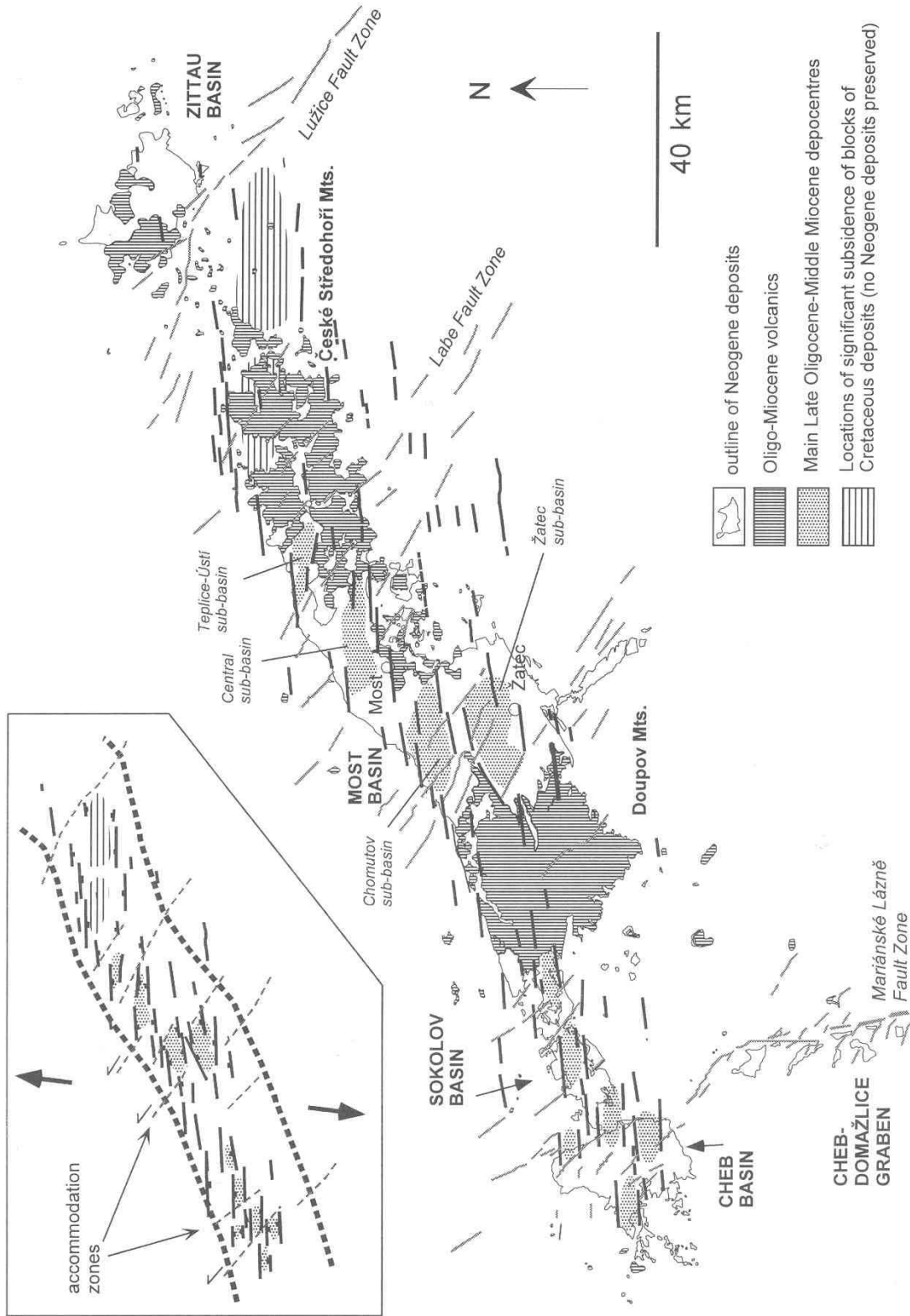


Fig. 1. A highly simplified map showing the positions of main depocentres in the Ohře Graben basins during the main phase of extension. For clarity, the NE-striking bounding faults (the Krušné hory and Ohře Fault zones), which formed later, are not shown.

sin became incorporated in the sharply kinked trace of the younger Krušné Hory Fault, formed under NW-oriented extension. It is clear that the Krušné Hory Fault is a composite structure, in places formed by hard linkage of older fault segments, and elsewhere comprising only monoclinical tilting of the basin-fill strata, including the main seam (Kopecký et al. 1985 and references therein). We suggest that this occurred in the locations of the original relay ramps. Although we admit that the rift-marginal faults in oblique-extensional regimes can propagate and merge with increasing extension under the same stress conditions, we believe that the differences in surface trends of the individual segments of the Krušné Hory Fault are large enough to justify our hypothesis of overprinting by reorientated extension vector. The length and straightness of the fault segments, and a high degree of connectedness of the Krušné hory and Ohře Fault Zones suggest that during their formation, the extension vector was orientated generally normal to the extension axis (cf. McClay and White 1995), which corresponds to the post-Lower Miocene period of NW-SE extension interpreted by Adamovič and Coubal (1999).

### The Bílina delta: main features of delta evolution inferred from large-scale depositional geometries

The Bílina Delta is a package of fluvio-deltaic clastics deposited during the early Miocene at the southeastern margin of the central sub-basin of the Most Basin (Fig. 3). The delta formed at the mouth of a river that drained into a fairly shallow lake (not more than several metres deep), which formed on a subsiding mire and was surrounded by peat bogs during most of the time of deltaic sedimentation (Dvořák and Mach 2000). The delta overlies the main coal seam in this part of the basin and a package of lacustrine clays (Fig. 3a). The mire which filled the basin prior to the deposition of deltaic clastics extended beyond the recent position of the Bílina Fault. The activity of the faults now bounding the sub-basin was both syn- and post-depositional.

The fluvial feeder system of the delta delivered sediment into the sub-basin from the east (Dvořák and Mach 2000), and a combination of flooding and onset of clastic input caused subsidence of a part of the mire, mostly under the load of water and abundant fine clastics. At the present stage of research, the cause of the onset of deltaic deposition remains speculative. One possible explanation is a propagation of E-W-striking extensional fault(s) from the east which caused an increase in subsidence in part of the sub-basin, and, at the same time, allowed the clastic sediment pathway to be established, probably along a relay ramp inclined to the west (cf. Peacock and Sanderson 1994; McClay and White 1995; Leeder and Gawthorpe 1990; Gupta et al. 1999). The westward direction of clastic supply, which supports this interpretation, followed the westerly dip of the pre-depositional surface, confirmed by mapping of stratal units in the vicinity of the Bílina Mine (K. Mach, unpublished data).

The main characteristic of the evolution of the Bílina deltaic system, according to Dvořák and Mach (2000), is the co-existence of the lake into which the delta prograded, and a mire which surrounded the lake margins over most of the delta lifetime (although the extent of the actively growing mire gradually decreased). Dvořák and Mach (2000) distinguished several phases of progradation of deltaic bodies, interrupted by flooding episodes. A significant part of accommodation was created by compaction of the underlying peat, and, during later parts of

the delta evolution, also by the compaction of lacustrine and prodelta clays (Fig. 3a).

In long term, the delta shows an overall trend of filling the accommodation space, which results in upward-increasing dominance of delta-plain and channel deposits over mouth-bar and prodelta deposits which dominate the lower portion of the section (for details see below). As the cross-section in Fig 3a runs approximately perpendicular to the general direction of sediment input, the stacking pattern observed in the Bílina section shows lateral shifting of the depositional system through time. During its evolution, the main site of deposition of coarse clastics shifted systematically north, which was driven by two factors: syndepositional tilting of the basement in the vicinity of the Bílina Fault (documented below) and the availability of compactible substrate north of the previously deposited deltaic bodies, which have already depleted the compaction potential of the underlying coal and clays. The beginning of deposition of lacustrine clays of the overlying Libkovice Member (Figs. 2,3) marks the final drowning of the Bílina delta system.

### Sedimentary environments and processes

Wedge-shaped and lenticular bodies of the delta sediments interfingering with the surrounding sheet-like bodies of lacustrine clays characterized the basic depositional pattern of the fluvio-deltaic depositional system (Fig. 3). Four fundamental architectural elements (Fig. 4), characterized also by distinctive associations of lithofacies, occur in the Bílina Delta proper: (i) fluvial and delta-plain heterolithic sheets, (ii) fluvial feeder channels with sand-dominated fills, (iii) sand mouth-bar wedges

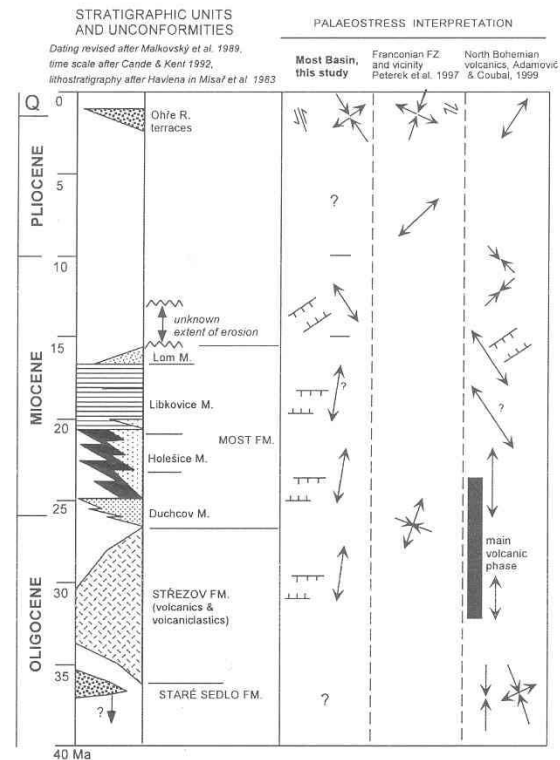


Fig. 2. Stratigraphic evolution of the Most Basin related to tectonic events.

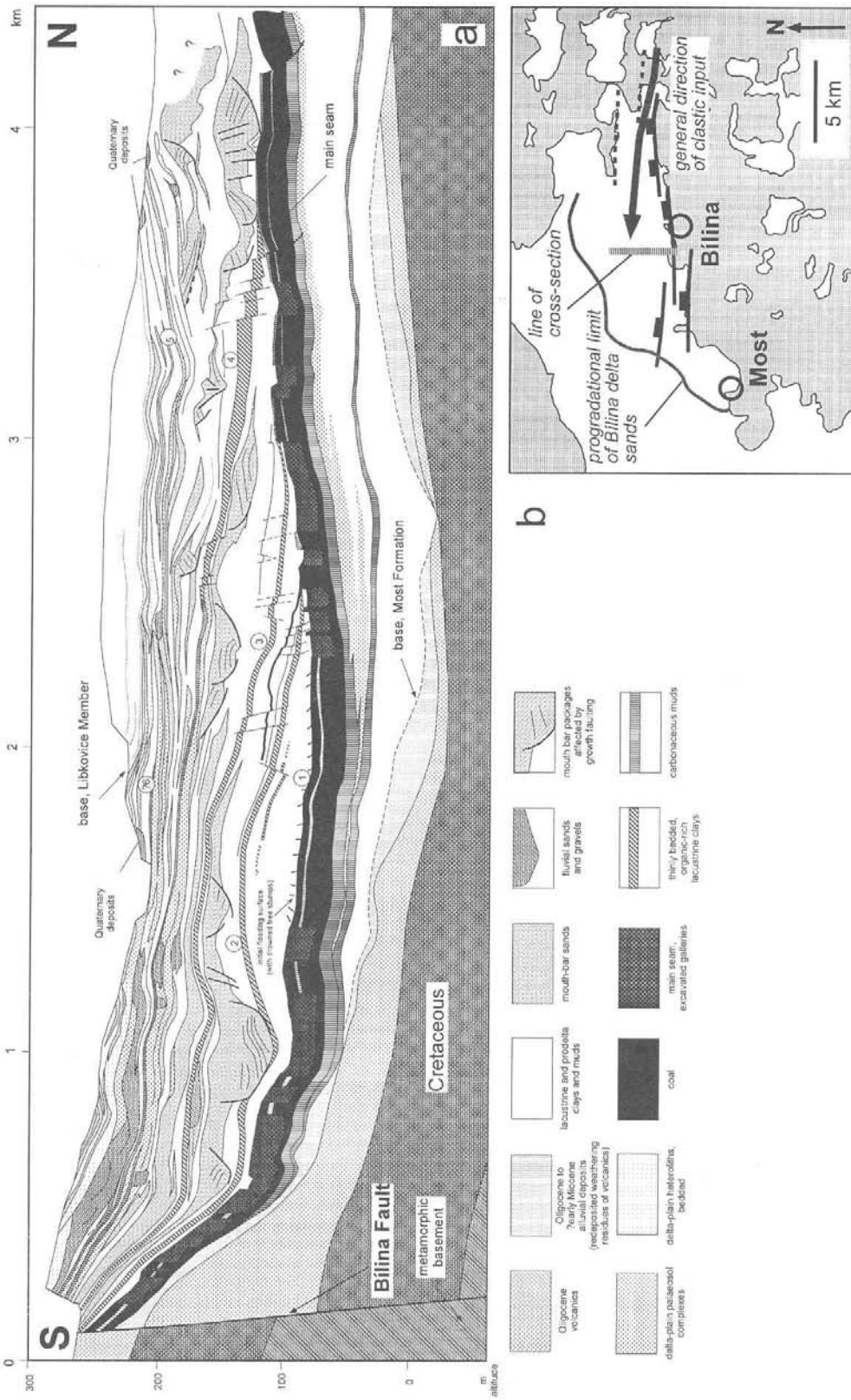


Fig. 3. (a) A N-S vertical cross-section of the Bilina Mine area, adapted from Dvořák and Mach (2000). Constructed from documentation of highwalls of the open-cast mine between 1981 and 1996. Circled numbers 1-6 refer to the maximum flooding intervals and their correlative surfaces in proximal facies (see text for details). (b) regional framework of the area of deposition of the Bilina Delta, and the location of the cross-section shown in (a). Note that the cross-section runs approximately perpendicular to the general direction of sediment input.

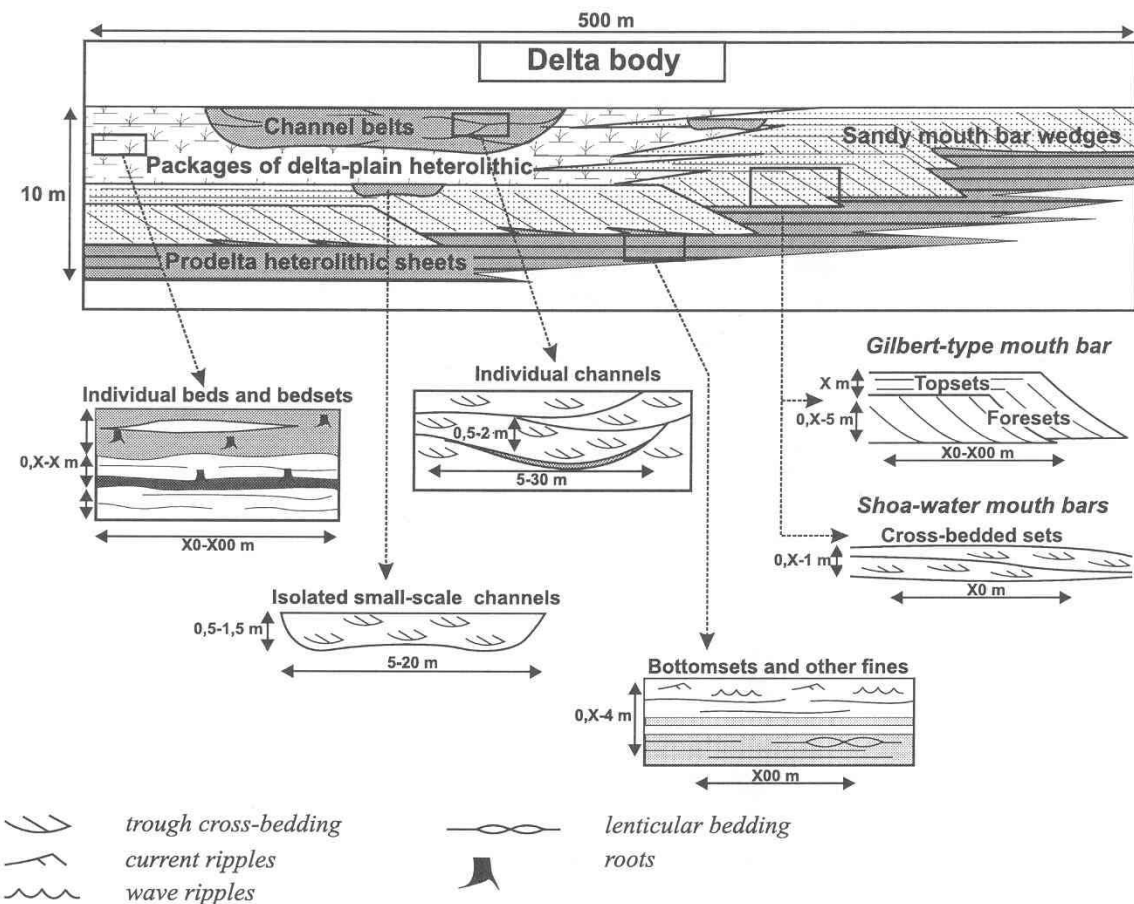


Fig. 4. Hierarchical scheme showing the relationship between individual architectural elements in the Břilina Delta depositional system.

es, and (iv) prodelta heterolithic sheets. Individual lithofacies (Fig. 5) represent individual sedimentary environments with specific sedimentary processes. The following brief review is based on Rajchl (1998) and Rajchl and Uličný (1999); for more details, the reader is referred to these studies.

The Břilina Delta is interpreted as a fluvial-dominated, mouth-bar type (or „birdfoot“) delta, with distributaries terminated by friction-dominated mouth bars, mostly with a Gilbert-type profile and a fan-like plan-view shape, characterized by steep, sandy foresets (Figs. 6,9). Locally, the mouth bars have a shoal-water profile free of foresets (Fig. 6). Larger distributaries were terminated by more complex subdeltas, consisting of a number of individual mouth bars, some probably contemporaneously active. The combined thickness of the foresets of the Gilbert-type mouth bars and thickness of the subaqueous portion of the topsets, formed in a few centimetres of water, indicate the depth of the receiving lacustrine basin not higher than c. 2–4 m at the delta front. The shoal-water mouth bars formed in water depth of c. 1 m or less.

The distributaries of the Břilina Delta feeder system are characterized by a large number of preserved channel fills. Based on differences in scale, we distinguish two types of channels: (i) large-scale channels (50–100 m wide) always comprising a number of nested, smaller channels (5–30 m) represent laterally migrating, braided channel belts; (ii) isolated, small-scale

channels (5–20 m) are interpreted as individual distributaries which acted as feeder channels of sand mouth bars. Three-dimensional reconstruction of individual channel paths (Mach, unpublished data) shows relatively straight traces of major channels, which indicates a lack of meandering.

A significant feature of the Břilina Delta is the high degree of separation of grain size in the lithosomes of the depositional system: the delta plain and prodelta were dominated by muddy lithologies, with a subordinate proportion of heterolithic facies (e.g., crevasse splay sands, or sand/mud laminites in the prodelta, traceable into mouth bar foresets), whereas the feeder channels and Gilbert-type mouth bars were dominated by sands. The small depth of the lake, and probably a very small difference in density between waters of the fluvial feeder system and the fresh-water lake are interpreted as having caused the high degree of grain-size segregation, as well as the formation of Gilbert-type foresets in a shallow setting that lacked topographic breaks, normally associated with steep, Gilbert-type delta fronts. Homopycnal, turbulent jets were probably the main type of effluent at the distributary mouths: turbulent mixing and deceleration at the distributary mouth caused the instant deposition of coarse material on the foresets. During time intervals when the river carried a much higher proportion of suspended load, the interaction of the effluent and the lake water was probably hypopycnal, causing formation of turbidity underflows. Alterna-

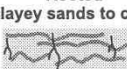
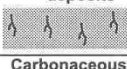
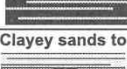
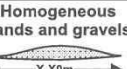
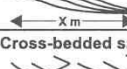
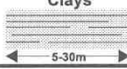
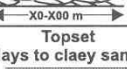
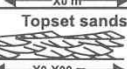
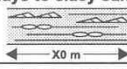
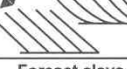
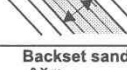
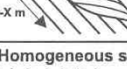

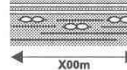



	<i>Lithofacies</i>	<i>Lithology</i>	<i>Sedimentary structures and other features</i>	<i>sedimentary processes</i>	<i>interpretation</i>	
<b>FLUVIAL AND DELTA PLAIN HETEROLITHIC SHEETS</b>	<b>Rooted clayey sands to clays</b> 	clayey sand to silt, sandy clay	sandy lamination, lenticular bedding; structures are deformed by roots	sedimentation from suspension dominant; occasional ripple migration	periodically flooded delta plain	
	<b>Rooted homogeneous deposits</b> 	silty clay to silt, (clayey fine sand)	homogeneous, rooted, with slickensides	intense pedogenesis	delta-plain palaeosols	
	<b>Carbonaceous clays to coals</b> 	dark clay rich in plant detritus, coal	horizontal stratification, deformation by roots	plant detritus accumulation	swamps of delta plain	
	<b>Clayey sands to clays</b> 	silty clay to silt, clayey fine sand	laminae of sand, lenticular bedding, wavy bedding, wave ripples	sedimentation from suspension alternating with tractional current	delta-plain lakes, interdistributary bays	
	<b>Homogeneous sands and gravels</b> 	fine-grained gravel, coarse to medium-grained sand	homogeneous, cross bedding	progradation of fan-like bodies; bedforms migration	crevasse splays	
<b>FLUVIAL CHANNELS (type I and II)</b>	<b>LA sands</b> 	coarse-grained sand to fine grained gravel	cross bedding	lateral accretion	point bars and peripheral bars ( distributary feeder system)	
	<b>Cross-bedded sands</b> 	fine-grained sand to fine-grained gravel	trough cross-bedding, current ripples	bedforms migration	active distributaries	
	<b>Clays</b> 	Silty clay to very fine-grained clayey sand	planar stratification; U-shaped fill	sedimentation from suspension	episodes of channel abandonment	
<b>SANDY MOUTH BAR WEDGES</b>	<b>shoal-water</b>	<b>Topset sands</b> 	medium to coarse-grained sand	trough cross-bedding, current ripples (locally climbing)	bedforms aggradation	active subaqueous delta plain
		<b>Topset clays to clayey sands</b> 	- silty clay to silt - clayey fine-grained sand	- lenticular bedding, laminae of sand - current and wavy ripples	sedimentation from suspension	inactive subaqueous delta plain
	<b>Gilbert-type</b>	<b>Topset sands</b> 	medium to coarse-grained sand	trough cross-bedding, current ripples (locally climbing)	bedforms aggradation	active subaqueous delta plain
		<b>Topset clays to clayey sands</b> 	- silty clay to silt - clayey fine-grained sand	- lenticular bedding, laminae of sand - current and wavy ripples	sedimentation from suspension	inactive subaqueous delta plain
		<b>Foreset sands</b> 	fine to medium-grained sand	inverse grading, homogeneous fabric	grain flow, grainfall; sedimentation from turbidity underflows	active delta front
		<b>Foreset clays</b> 	silty clay to silt, clayey very fine-grained sand	draping planar stratification	sedimentation from suspension	inactive delta front
		<b>Backset sands</b> 	fine to medium-grained sand	upslope-dipping cross-lamination, filling spoon-shaped scours	upslope migration of hydraulic jump	active delta front
		<b>Homogeneous sands</b> 	fine to medium-grained sand	homogeneous fabric	sliding and slumping on delta front	delta front
<b>PRODELTA HETEROLITHIC SHEETS</b>	<b>Heteroliths</b> 	clayey fine sand to sandy clay to silty clay	current and wave ripples, flaser bedding, wavy bedding, lenticular bedding, planar lamination	sedimentation from turbidity currents and suspension	prodelta: bottomsets of mouth bars, other fines	

Fig. 5. Overview of individual lithofacies and their interpretation.

tion of homo- and hyperpycnal conditions can be interpreted in outcrops from alternation of sharp-based, inversely graded foresets (representing the homopycnal conditions characterized by grainflows), with foresets showing a tangential transition into heterolithic bottomsets characterized by homogeneous or normally-graded laminae, interpreted as turbidite deposits. Frictional effects due to the very small depth of the receiving basin caused a very rapid lateral expansion of the jets, leading to the fan-like geometry of the mouth bars in plan view.

### Syn depositional deformation

A range of types of syn depositional, ductile and brittle deformation structures ranging in scale from centimetres to metres to tens of metres occur in the sediments of the Bílina Delta (Rajchl 1999; Rajchl and Uličný 1999). Based on their scale, we distinguish between small-scale deformation structures, which affect only parts of the mouth bars, and large-scale deformation structures affecting whole mouth bars or their packages (Fig. 7). The syn depositional deformation structures could have been caused either by allogenic processes (e.g., seismicity), or by autogenic processes resulting from the evolution of sedimentation within the prograding delta system.

The most important small-scale structure is convolute bedding which occurs in sets of diagonal stratification – in the Gilbert-type foresets of mouth bars as well as in cross-bedded channel fills. This structure is represented by folding of original foresets to broad synclines and sharp anticlines. Fold planes are commonly overturned in the direction of the original dip of stratification. The formation of these structures was induced by rapid loss of stability of the original sedimentary structure by liquefaction of the whole foreset package and subsequent repacking of grains into a more stable configuration. The sharp anticlines were caused by upward water escape induced by fluidi-

zation which often follows liquefaction. Breaching of the anticlines in their tips and fluid-escape structures are also common. Main processes capable of inducing the liquefaction in these cases are (i) earthquakes causing liquefaction followed by slope failure, (ii) unequal surface loading by an overlying sediment body, or (iii) action of both processes combined.

Folded and fractured topsets occur in association with the above structure. Original structures of sandy topsets (active subaqueous delta-plain sediments) and interbedded thin clay layers (passive subaqueous delta-plain sediments) are folded to broad synclines and narrow anticlines. Internal folding of sand topsets was caused by the liquefaction of the whole topset, commonly accompanied by fluidization. The clay layers folded in response to liquefaction of the surrounding sand. In case of more intense deformation, the folded clay layers were breached in the anticlinal tips where fluid escape structures formed. Thicker clay layers were fractured without folding and their fragments sank into the liquefied sand. The main triggering processes were probably either seismic activity or over-pressuring by overlying sedimentary bodies, or both.

The largest syn depositional deformation structures are growth faults, characterized by listric fault planes and systematic stacking of a higher number of mouth bars on hangingwall side (Figs. 7, 8). The growth faults occur only within delta bodies underlain by a thick accumulation of clay and/or the coal seam. During the evolution of the Bílina Delta, the locations of thick sandbodies affected by growth faulting show a systematic shift to places with compaction potential of significant underlying thickness of clays and/or coal (Fig. 3). The origin of the growth faults is generally attributed to differential loading of easily deformable mobile substrate, such as lacustrine clay, coal, or prodelta heteroliths (e.g., Bruce 1973; Morley and Guerin 1996). The formation of accommodation needed for aggrada-

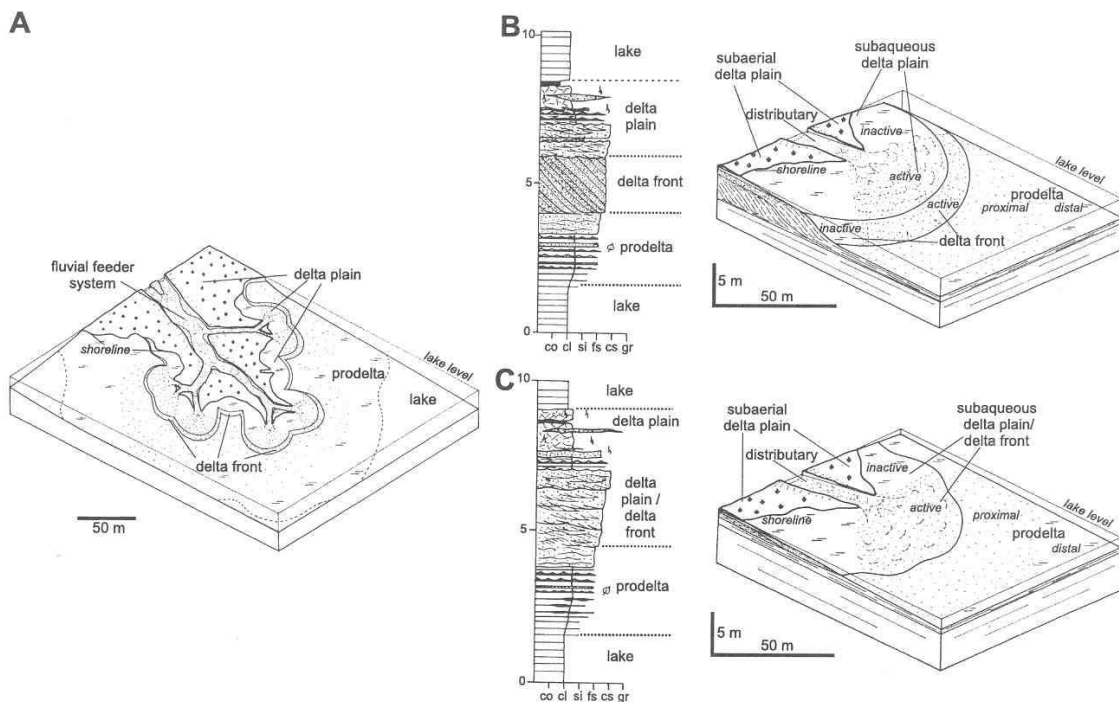


Fig. 6. A – hypothetical model of the Bílina Delta; B – model of a Gilbert-type mouth bar; C – model of a mouth bar with a shoal-water profile.




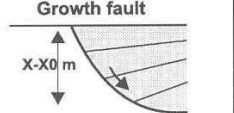
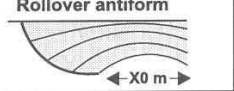



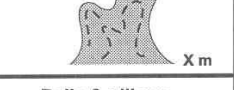

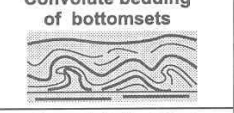
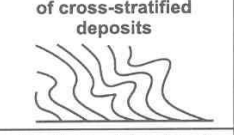


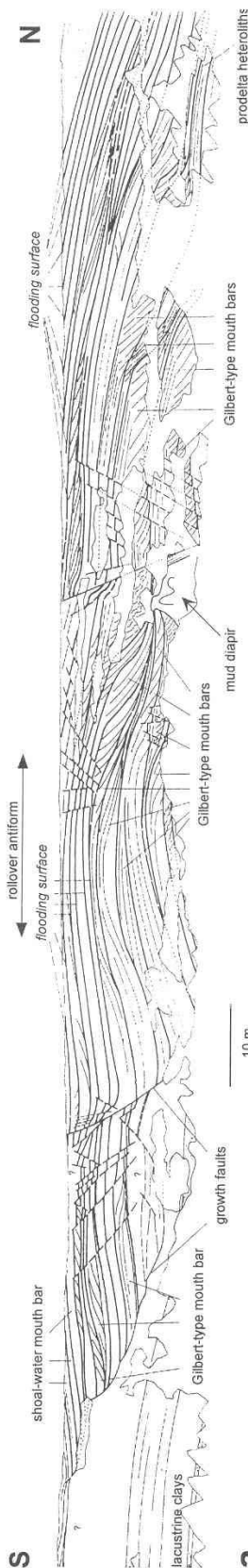
	<b>structures</b>	<b>description (occurrence)</b>	<b>mechanism of deformation, triggering processes</b>
<b>LARGE-SCALE STRUCTURES</b>	 <p><b>Compactional sag</b></p>	sagging of mouth bars and distributary channel fills	compaction due to loading of unconsolidated plastic sediments by rapidly deposited sand bodies
	 <p><b>Growth fault</b></p>	fault with listric shaped plain characterised by high number of vertically stacked mouth bars on hangingwall side	brittle deformation resulting from differential loading of easily deformable, mobile substrate
	 <p><b>Rollover antiform</b></p>	bulged anticline-like structure made from package of mouth bars affected by growth faulting	rotation of hangingwall block of a listric growth fault
	 <p><b>Normal faults</b></p>	normal faults situated in antiform apex or in areas of compactional sagging	response to localized extension (e.g. in the apex of rollover antiform) or overburdening
	 <p><b>Thrusts</b></p>	brittle compressional structures situated near delta bodies affected by growth faulting; always occur in the footwall	outward migration of overpressured material
	 <p><b>Folds</b></p>	ductile compressional structures situated on the periphery of delta bodies affected by growth faulting; always occur in the footwall	outward migration of overpressured material
	 <p><b>Mud diapirs</b></p>	body of mobilized plastic material piercing overlying sediments	upward migration of overpressured material
<b>SMALL-SCALE STRUCTURES</b>	 <p><b>Balls &amp; pillows</b></p>	rounded and lobate structures at the base of sandy beds underlain by clayey beds (subaqueous delta plain, prodelta)	liquefaction of less dense substrate due to inverse density gradients; sinking of denser material  rapid loading of less dense sediment by denser sediment; seismic shaking
	 <p><b>Convolute bedding of bottomsets</b></p>	folding of primary lamination of sandy beds of proximal prodelta to broad synclines and sharp anticlines	plastic deformation of liquefied sediment, accompanied by fluidization  rapid sedimentation; seismic shock
	 <p><b>Convolute bedding of cross-stratified deposits</b></p>	folding, mainly of mouth bar foresets, to broad synclines and sharp anticlines	liquefaction and fluidization followed by repacking of grains into a more stable configuration  seismic shock; unequal loading; combination both
	 <p><b>Folded and fractured topsets</b></p>	folding of internal bedding of sandy topsets and folding of whole clayey topsets to broad syncline and sharp anticlines	liquefaction of whole set and fluidization  earthquakes; loading
	 <p><b>Fluid-escape structures</b></p>	fracturing of anticlinal tips in folded clay layers	upward escape of water and sand from liquefied and fluidised sand bed  earthquakes; loading

Fig. 7. Overview of deformation structures occurring in the Bilina Delta deposits, their deformation mechanisms and triggering processes.



**a** Fig. 8a. Example of a delta body affected by growth faulting.

tion of the mouth bars was governed by the following processes:

- (i) high compaction rate of overpressured sediments in response to pore-fluid migration induced by loading; this migration was accompanied by a downward rise of pore-fluid pressure which caused the flattening of growth faults with increasing depth;
- (ii) outward migration of the overpressured mobile substrate. The migration is revealed by the occurrence of ductile and brittle compressional structures (folding, thrusting) developed in prodelta heteroliths and lacustrine clays on the periphery of the delta bodies influenced by growth faulting. Mud diapirs also occur on the delta periphery, and the ascent of some of them led to piercing of the overlying delta bodies (Fig. 8b).

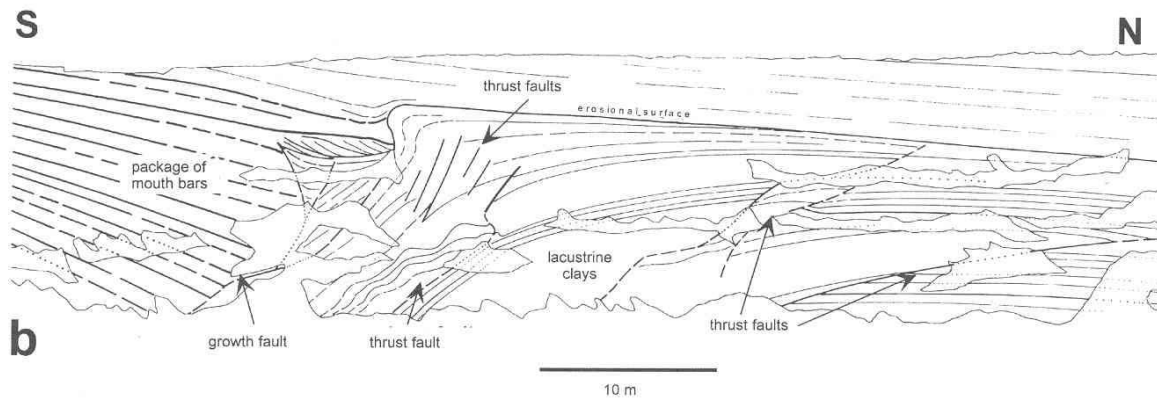
Delta bodies affected by growth faulting are characterized by high thicknesses and commonly by "pot" shapes. High subsidence on the delta body periphery (along the growth faults) and hangingwall-block rotation induced formation of a rolover antiform, with its axis situated approximately in the centre of the delta body. The thicknesses of mouth bars markedly decrease from the fault planes towards rolover antiforms formed by the rotation over the growth faults. The growth of the rolover antiform was accompanied by formation of an array of antithetic, en-echelon normal faults in the axial parts of antiforms in response to localized extension (Fig. 8a). Some of these faults could have become active also later as younger growth faults or as ascent paths for shale diapirs.

### Sequence-stratigraphic aspects

The deltaic deposits recorded a large number of changes in accommodation, at various time scales and of varying orders of magnitude. The accommodation in the lacustrine-deltaic system was controlled by a combination of factors, which include (i) tectonic subsidence and uplift, (ii) compaction of peat and mud and related syndepositional deformation (e.g., growth faulting), and (iii) climate-driven absolute lake-level changes. At the present stage of research we can separate two groups of relative lake-level changes, resulting from combination of the above controls: (1) low-frequency changes, presumably in the order of first tens of metres, recorded by changes in depositional patterns in the whole depositional system, and (2) high-frequency, in the order of metres to even fractions of one metre, recorded at the level of individual mouth bars or groups of mouth bars (subdeltas; Rajchl and Uličný 1999).

**1. The low-frequency relative lake-level changes** are interpreted to have controlled the development of 5 to 6 low-frequency sequences, characterized by alternating transgressive and regressive episodes. Because of the high rate of increase in accommodation by compaction, it is difficult to find clear evidence of a significant relative lake-level fall and formation of a typical sequence boundary (sensu Van Wagoner et al. 1988) of the corresponding order. Therefore, we cannot apply the classical Exxon scheme of 3 (or 4) systems tracts – instead, we use a simplified scheme which employs a division into Transgressive and Regressive systems tracts, separated by a maximum flooding interval. This approach is closer to the genetic stratigraphy of Galloway (1989).

The main features of low-frequency sequences in the Bilina system can be summarized as follows: early transgressive systems tract (TST) is characterized by aggradation of delta-plain deposits, including carbonaceous muds, on top of mouth-bar



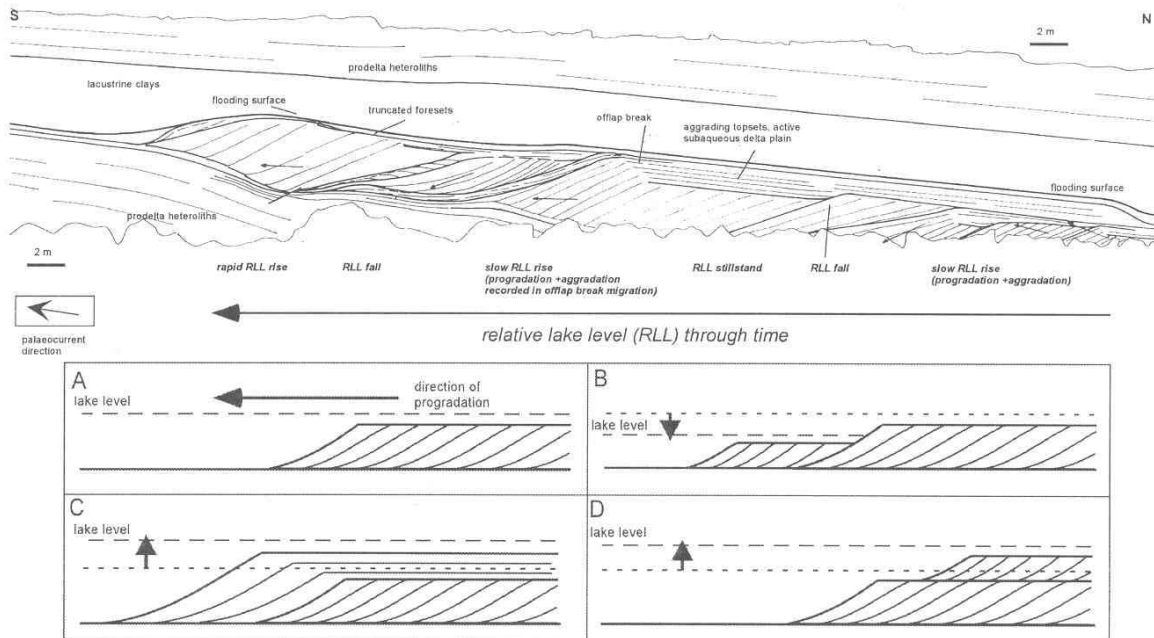
**Fig. 8b.** Compressional structures on the periphery of the delta body affected by growth faulting. (Direction of progradation of the mouth bars is away from the viewer.)

sands and also on top of distributary channel fills. A lacustrine flooding surface on top of the delta-plain deposits marks the onset of lacustrine deposition of late TST; locally it shows signs of wave reworking of underlying deposits. A maximum flooding interval is characterized by deposition of organic-rich, laminated muds. This interval is overlain by thick deposits of the regressive systems tract (RST), which is volumetrically more significant than the TST, because it contains progradational deltaic clastics characterizing the period of increasing ratio between the rate of deposition and rate of accommodation increase.

In the uppermost parts of the Bilina section, where proximal

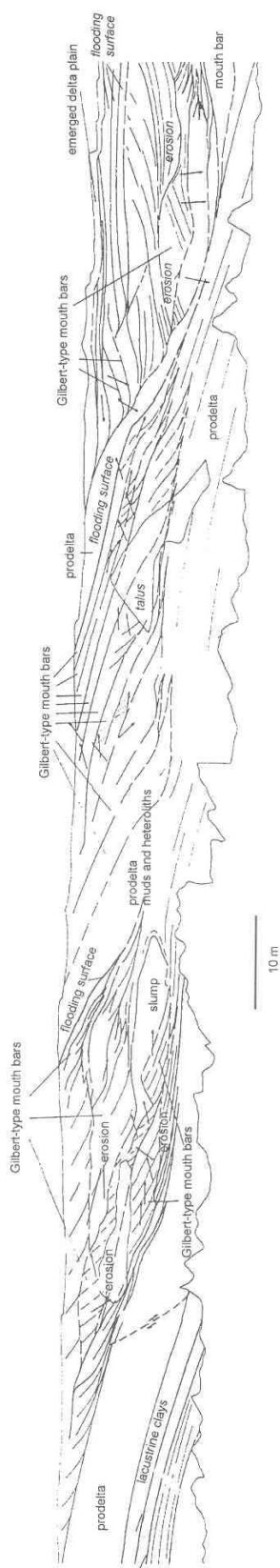
facies prevail, several sequences may be amalgamated in a complex of palaeosols, channel fills and thin mouth bars. These sequences would have been deposited to the west of the Bilina region, which was characterized by bypass of sediment over the filled sub-basin during their deposition. During high relative lake-level intervals, lacustrine facies were never deposited here and carbonaceous muds interbedded with the palaeosols may represent proximal expression of maximum flooding intervals (cf. Flint et al. 1995).

The influence of compaction on the geometry of the sequences is expressed in the lateral migration of the sequences



**Fig. 9.** Cross-section of a part of a subdelta showing reactions of a Gilbert-type mouth bar to a series of relative lake-level changes during progradation. Inset: types of response of mouth bars to relative lake-level changes.

**A** – progradational pattern of a mouth bar during stable lake level; **B** – reaction of a mouth bar to a relative lake-level fall (forced regression); **C** – progradational pattern of a mouth bar during a relative lake-level rise – rate of sediment input is higher than rate of relative lake-level rise, which results in topset aggradation coeval with progradation; **D** – rate of relative lake-level rise was significantly higher than rate of sediment input – the upper mouth bar formed after subsequent stabilization of lake level.



**Fig. 10.** Cross-section showing syndepositional tilting of the basement recorded in different slopes of individual delta bodies (best shown by the flooding surfaces covering the topsets, which were closest to horizontal at the moment of formation). See comments in text.

in the Bílina section. Fig. 3a clearly shows that the younger deltaic bodies successively onlap on the seam, in northern direction, where unused compaction potential still existed. This pattern is marked by the beds of dark lacustrine clays, interpreted as maximum flooding intervals. During periods of high relative lake level, the mire was flooded over a larger area than represented in the Bílina Mine, and the dark lacustrine clays are traceable into clayey interbeds in the uppermost part of the seam (Dvořák and Mach 2000). We infer that the low-frequency relative lake-level changes resulted from the interplay between tectonic subsidence and climatic events; compactional subsidence acted against any potential rapid falls in relative lake level. Dvořák and Mach (2000) suggest that the fluctuations in clastic input may have controlled much of the accommodation fluctuations by changing the rate of loading of the compactible substrate.

The drowning event which marks the termination of deposition in the Bílina Delta and is marked by the onset of deposition of the Libkovic Member lacustrine clays, occurred approximately during the same time as the onset of deposition of the Cypris mudstones in the Sokolov and Cheb Basins, and we tentatively interpret it as caused by increase in subsidence rate in the whole Eger Graben system. In the uppermost parts of the Bílina Mine, a succession of thin, wide, Gilbert-type mouth bars, arranged in a retrogradational stacking pattern, is interpreted as a low-frequency transgressive systems tract of another sequence, corresponding to the Libkovic Member. These clastic wedges recorded the last phases of deltaic deposition in this area, before the rate of relative lake-level rise prevailed over the rate of sediment input.

**2. High-frequency relative lake-level changes** can be recognized in the internal geometries and stacking patterns of individual mouth bars, which were sensitive recorders of small-scale, short-term changes in accommodation. We infer that a major control on the high-frequency sequences was represented by climatically induced changes in lake level, because the deposition of individual mouth bars in depth of less than 5 m probably occurred at time scales of tens to hundreds of years. Rapid compactional subsidence and tectonic effects modified the geometries of the mouth bars. Relatively slow changes in accommodation (relative to the rate of deposition) were recorded as changes in the progradation vs. aggradation rates, expressed mostly as changes in topset thickness and position of the offlap break (Fig. 9). More rapid changes in relative lake level caused formation of flooding surfaces on top of drowned mouth-bar bodies and delta-plain deposits in case of lacustrine transgression, or deposition of foresets capped by a bypass or erosional surface, interpreted as a result of forced regression.

Geometric relationships between individual Gilbert-type mouth bars reveal subtle but important reactions of the mouth bars to changes in the basin-floor behaviour. Figure 10 shows that a succession of mouth bars near the Bílina Fault was affected by syndepositional tilting, unrelated to compaction, which is detected from uniform tilting of the flooding surfaces in the earlier mouth bars (left-hand side of the figure). The deposition of a new mouth bar, following the tilting episode, took place on the northern side of the older mouth bar, with more compactible substrate available. The loading then caused partial deformation of the new mouth bar, as well as further tilting of the adjacent part of the older mouth bar. A number of successions like this occur within a c. 400 m wide interval to the north of the Bílina Fault and suggest that propagation of an extensional fault in the subsurface – possibly a precursor of the present-day

Bílina Fault – caused northward tilting of the basement prior to brittle failure and subsidence of the hangingwall (cf. Gupta et al. 1999). The syndepositional tilt of the basement near the Bílina Fault is also implied by the systematic northward shift of large-scale deltaic bodies throughout the section.

Another important feature in the high-frequency sequences is related to the syndepositional subsidence in the hangingwalls of growth faults. Rotation of the hangingwall block on the listric fault plane causes not only an increase in thickness of a mouth bar towards the fault, but can also lead to temporary flooding if the subsidence along the fault is too rapid for the mouth bar to remain at the water level. At several locations, we observed amalgamation of flooding surfaces toward the apex of the rollover antiform. This shows that flooding surfaces can form purely by rapid subsidence above a growth fault. Vertical repetition of such surfaces within a stack of mouth bars suggests an episodic nature of the movement along the faults, which was probably driven, or at least influenced, by the rate of loading. Therefore, we infer that, as in the case of the low-frequency sequences, an increase in the rate of sediment input caused, paradoxically, a penecontemporaneous increase in accommodation.

## References

- ADAMOVIČ J. and COUBAL M., 1999. Intrusive geometries and Cenozoic stress history of the northern part of the Bohemian Massif. *Geolines*, 9: 5-14.
- BLÍŽKOVSKÝ M., MAŠÍN J., MÁTLOVÁ E., MITRENGA P., NOVOTNÝ A., POKORNÝ L., REJL L. and ŠALANSKÝ K., 1988. Lineární struktury čs. části českého masívu podle geofyzikálních indikací. *Věstník ÚÚG*, 63: 275-290.
- BRUCE C. H., 1973. Pressured shale and related sediment deformation: mechanism for development of regional contemporaneous faults. *AAPG Bulletin*, 57: 878-886.
- CAJZ V., VOKURKA K., BALOGH K., LANG M. and ULRYCH J., 1999. The České středohoří Mts.: volcanostratigraphy and geochemistry. *Geolines*, 9: 21-28.
- CANDE S. C. and KENT D. V., 1992. A new geomagnetic polarity time scale for the Late Cretaceous and Cenozoic. *Journal of Geophysical Research*, 97, B10: 13917-13951.
- DVOŘÁK Z. and MACH K., 2000, in print. 15 let dokumentace miocenních sedimentů na dole Bílina. *Acta Universitatis Carolinae*.
- FLINT S., AITKEN J. and HAMPSON G., 1995. Application of sequence stratigraphy to coal-bearing coastal plain successions: implications for the UK Coal Measures. In: WHATLEY M.K. and SPEARS D.A. (Editors), *European Coal Geology*. Geological Society Special Publication 82, 1-16.
- GALLOWAY W. E., 1989. Genetic stratigraphic sequences in basin analysis I: Architecture and genesis of flooding-surface bounded depositional units. *AAPG Geologists Bulletin*, 73: 125-142.
- GUPTA S., UNDERHILL J. R., SHARP I. R. and GAWTHORPE R. L., 1999. Role of fault interactions in controlling syn-rift sediment dispersal pattern: Miocene, Abu Alaqa Group, Suez Rift, Sinai, Egypt. *Basin Research*, 11: 167-189.
- HURNÍK, S. 1959. Prvé zjištění cyklické sedimentace v terciálních limnických pánvích ČSR. *Věstník ÚÚG*, 34: 269-278.
- HURNÍK, S. 1978. Deltová sedimentace v severočeské hnědouhelné pánvi. Sborník 3. uhel. geol. konference, PřF UK, Praha, 89-94.
- KOPECKÝ L., 1978. Neoidic taphrogenic evolution and young alkaline volcanism of the Bohemian Massif. *Sborník geologických věd, Geologie*, 31: 91-107.
- KOPECKÝ L., KVĚT R. and MAREK J., 1985. K otázce existence krušnohorského zlomu. *Geologický průzkum*, 1985, 164-168.
- LEEDER M.R. and GAWTHORPE R.L., 1987. Sedimentary models for extensional tilt-block/half-graben basins. *Geological Society of London Special Publication*, 28: 139-152.
- MALKOVSKÝ M., BUCHA V. and HORÁČEK J. 1989. Rychlost sedimentace terciéru v mostecké části severočeské hnědouhelné pánve. *Geologický průzkum*, 1989, 2-5.
- McCLAY K. R. and WHITE M. J. 1995. Analogue modelling of orthogonal and oblique rifting. *Marine and Petroleum Geology*, 12: 137-151.
- MÍSAŘ Z., 1983. Geologie ČSSR I. Český masív. Academia, Praha, 325 pp.
- MORLEY C.K., CUNNINGHAM S.M., HARPER R.M. and WESCOTT W., 1992. Geology and geophysics of the Rukwa Rift, East Africa. *Tectonics*, 11: 69-81.
- MORLEY C.K. and GUERIN G., 1996. Comparison of gravity-driven deformation styles and behavior associated with mobile shales and salt. *Tectonics*, 15: 1154-1170.
- PEACOCK D.C.P. and SANDERSON D.J., 1994. Geometry and development of relay ramps in normal fault systems. *AAPG Bulletin*, 78: 147-165.
- PETEREK A., RAUCHE H., SCHRÖDER B., FRANZKE H.-J., BANKWITZ P. and BANKWITZ E., 1997. The late- and post-Variscan tectonic evolution of the Western Border fault zone of the Bohemian Massif (WBZ). *Geologische Rundschau*, 86: 191-202.
- RAJCHL, M., 1999. Structures due to synsedimentary deformation in sediments of the Bílina Delta (Miocene, Most Basin, Czech Republic). Proceedings of the 4th Meeting of the Czech Tectonic Studies Group, *Geolines*, 8: 57.
- RAJCHL M. and ULIČNÝ D., 1999. Sedimentární model bílinské delty. *Hnědé uhlí*, 3: 15-42.
- RAJCHL M. and ULIČNÝ D., 2000. Evolution of basin-fill geometries in the Most Basin: implications for the tectonosedimentary history of the Ohře Rift (Eger Graben), North Bohemia. Proceedings of the 5th Meeting of the Czech Tectonic Studies Group, *Geolines*, this volume.
- SENGÖR A.M.C., 1995. Sedimentation and tectonics of fossil rifts. In: BUSBY C.J. and INGERSOLL R.V. (Editors), *Tectonics of Sedimentary Basins*, Blackwell Science, Oxford, 53-117.
- ŠPIČÁKOVÁ, L. and ULIČNÝ, D., 2000. Tectonosedimentary history of the Cheb Basin (NW Bohemia). Proceedings of the 5th Meeting of the Czech tectonic Studies Group, *Geolines*, this volume.
- TRON V. and BRUN J.P., 1991. Experiments on oblique rifting in brittle-ductile systems. *Tectonophysics*, 188: 71-84.
- VAN WAGONER J. C., POSAMENTIER H.W., MITCHUM R.M., VAIL P.R., SARG J.F., LOUTIT T.S. and HARDENBOL J., 1988. An overview of sequence stratigraphy and key definitions. In WILGUS C.V. et al. (Editors), *Sea level changes: an integrated approach*. SEPM Special Publication 42, pp. 39-45.
- WILSON M., 1993. Magmatism and the geodynamics of basin formation. *Sedimentary Geology*, 86: 5-30.
- ZIEGLER P. A., 1990. Geological Atlas of Western and Central Europe. Shell Internationale Petroleum Maatschappij, The Hague, 239.

## DAY 2

### Introduction:

Recent research in the central part of the Krušné hory Mts. (Fig. 1) has radically changed the view on tectonic and metamorphic evolution of this area. Previous studies were focused on lithostratigraphic subdivision of this metamorphic complex but did not consider some important tectonometamorphic phenomena. Metamorphic zoning from the core of the Krušné hory Mts. towards the Paleozoic cover in the west is interrupted by the occurrence of large bodies of eclogite-facies rocks. Eclogites are surrounded by coarse- and fine-grained orthogneisses and several types of metasediments which form the four main structures of this area – the Klínovec anticline, the Měděnec anticline, the Měděnec syncline and the Oberwiesenthal structure (Fig. 2).

In the German part of the Krušné hory Mts., Willner et al. (1994) have proposed three major high-pressure (HP) units with decreasing metamorphic grade from the lowermost to the uppermost unit. Krohe (1996) interpreted this feature as a result of ductile extension during exhumation of the thickened Saxothuringian domain.

Our interpretation of the Czech part of the central Krušné hory Mts. will be demonstrated during the excursion. Lack of extensional structures in the studied area suggests that successive structural evolution is the result of compressional regimes acting in different orientations during the Variscan collision.

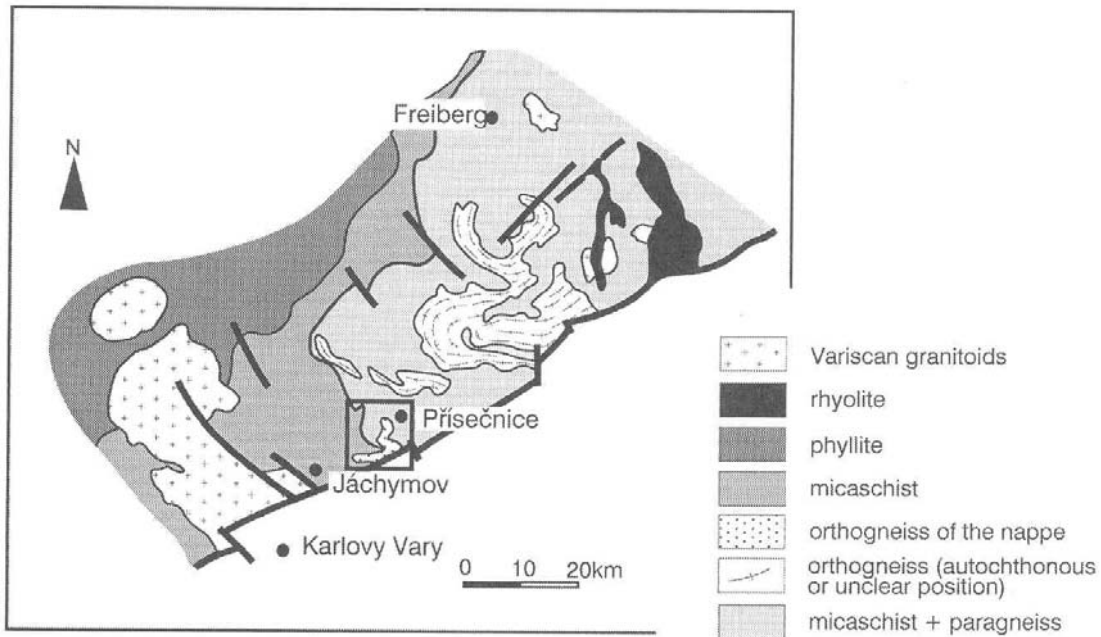


Fig. 1. Simplified geological map of the central part of the Krušné hory Mts.

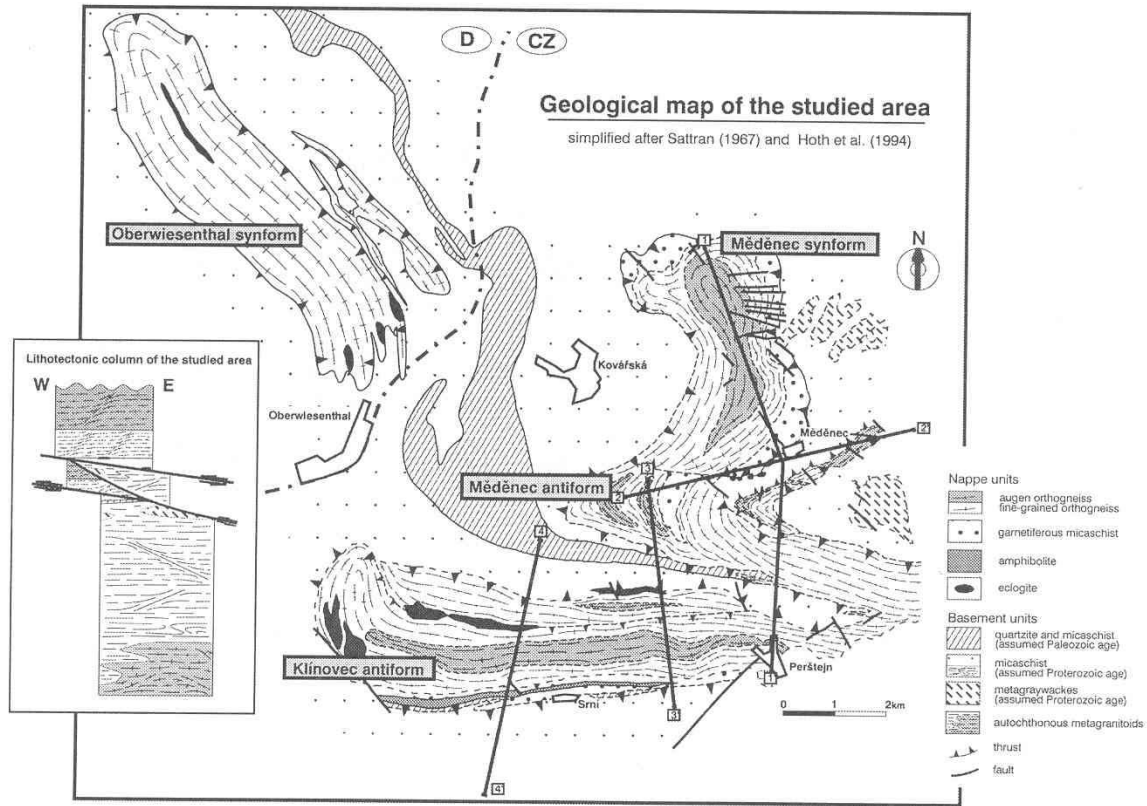


Fig. 2. Simplified geological map of the area studied. The left inset represents lithotectonic column of the studied area.

## Stop 1

### Cross-section from the basement to the core of the Měděnec synform

Jiří KONOPÁSEK and Karel SCHULMANN

The Měděnec synformal structure is developed north of the village of Měděnec and represents a key area for the interpretation of structural evolution of the central Krušné hory Mts. between Jáchymov and Přísečnice.

In the Měděnec synform, the main metamorphic foliation in all present rock types except eclogites appears to be the result of top-to-the-west oriented thrusting. This interpretation is

supported by both the E–W- to ESE–WNW-oriented  $L_2$  stretching lineation and the presence of the SC fabrics in coarse-grained orthogneisses. Gently dipping D2 fabric can be observed more or less in its original position being only slightly affected by late  $F_2$  folding resulting in synformal shape of the structure (Fig. 3).

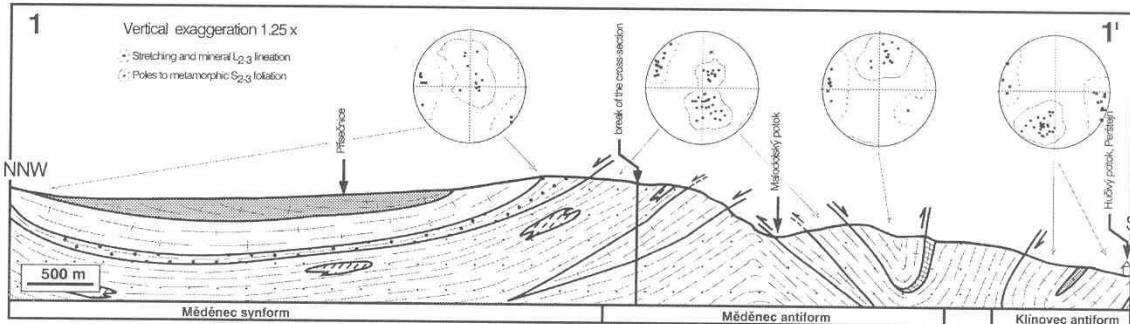


Fig. 3. Cross-section of the Měděnec synform and adjacent area with the D2-D3 structural data represented by the lower-hemisphere equal-area projection. Data are contoured at 1x uniform distribution. See Fig. 2 for the position of the cross-section and key to patterns of the rock types.

## Stop 1a

**Plagioclase schists** appear in structurally lowermost position of the section and represent the typical rock type of the Krušné hory Mts. autochthon. The rock itself is composed mainly of Ms + Bt + Chl + Qtz matrix with large plagioclase porphyroblasts (Fig. 4) and shows complicated polymetamorphic history. Samples from several localities bear those mineral assemblages which are enveloped in plagioclase porphyroblasts of typical plagioclase schists. The estimated metamorphic conditions of 600 °C and 14.5 kbar (Fig. 5) suggest that these samples represent the near-peak pressure stage and the assemblage corresponds to the PT conditions during main collisional event.

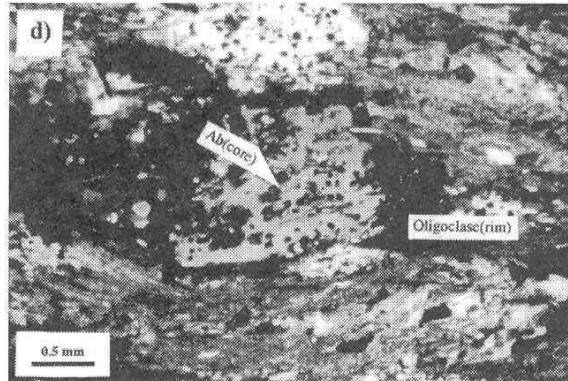


Fig. 4. Photomicrograph showing plagioclase porphyroblast in the matrix of typical plagioclase schists (from Konopásek 1998).

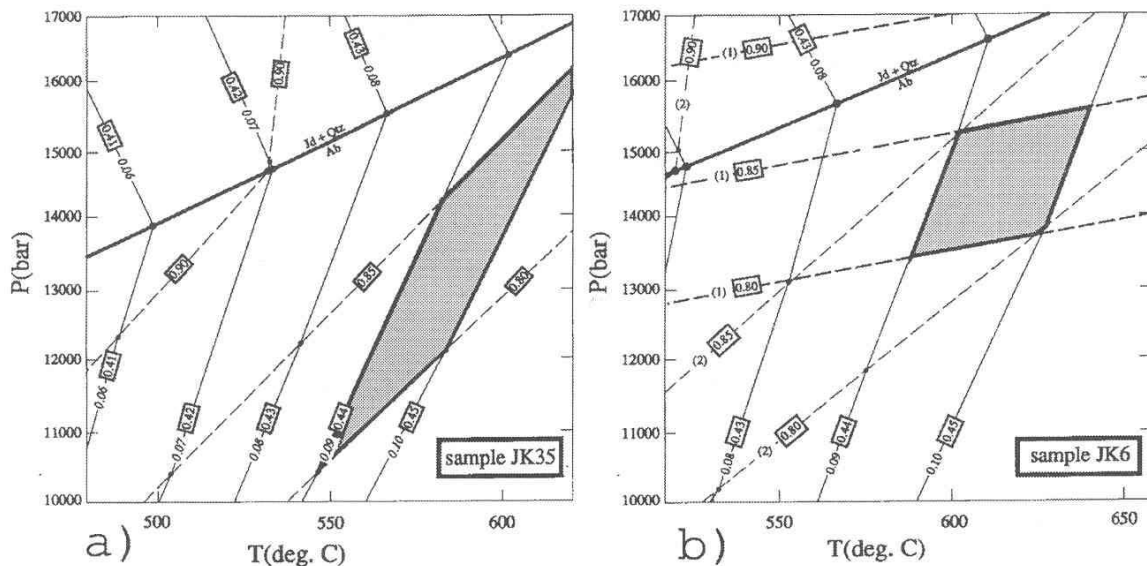


Fig. 5. PT estimates for the peak-pressure conditions in the basement metasediments (from Konopásek 1998).

## Stop 1b

**Garnetiferous (Měděnec) micaschists** appear as a distinct layer rimming the main orthogneiss body of the Měděnec synform. North of the village of Měděnec, garnetiferous micaschists are spatially associated with bodies of mafic eclogites. Micaschist itself consists of Ms + Pg + Ky + Qtz bearing matrix with Grt

porphyroblasts. Kyanite was observed in cores of garnet porphyroblasts, being stable with numerous crystals of chloritoid (Fig. 6). This assemblage yielded PT conditions of 580 °C at 14–15 kbar (Fig. 7) indicating that garnetiferous micaschists are not of the same facies as mafic eclogites.



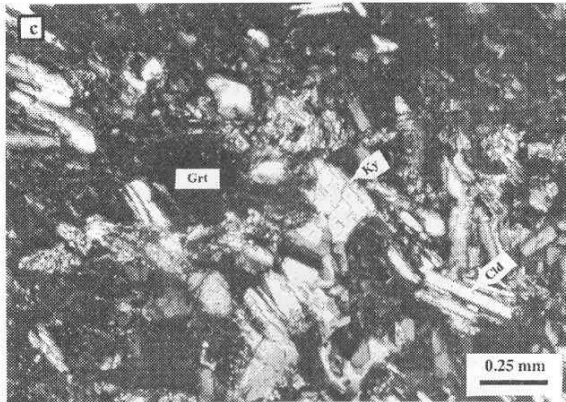


Fig. 6. Photomicrograph showing mineral assemblage Cld + Ky enveloped in a garnet porphyroblast from garnetiferous micaschist (from Konopásek in print).

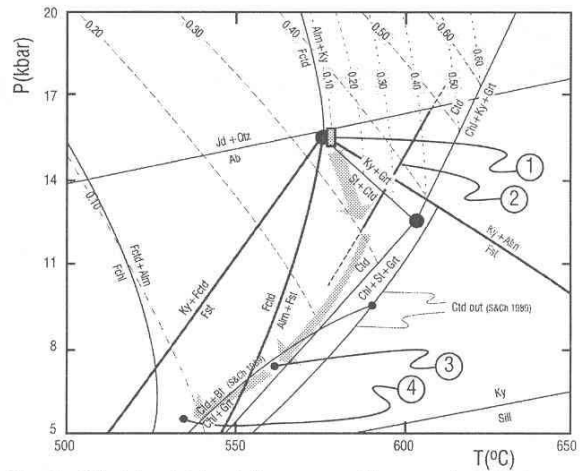
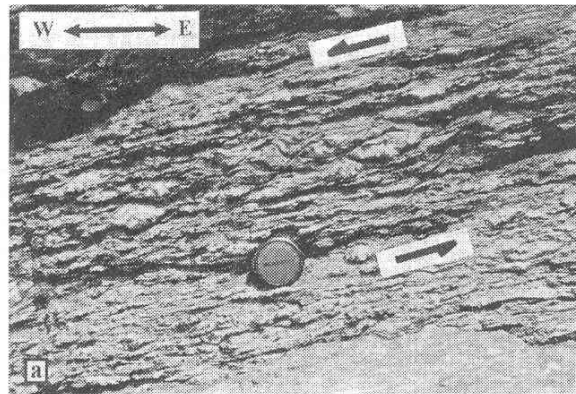


Fig. 7. PT data obtained from garnetiferous micaschists are marked by solid lines in calculated PT grid. The PT box (No.1) was established on the basis of composition of chloritoid ( $X_{Mg} = 0.07$ ) in the assemblage Grt–Cld–Ky, observed in the Měděnec micaschists.

### Stop 1c

**Fine-grained orthogneisses, augen orthogneisses and meta-granites** represent the core of the Měděnec synform. Stable mineral assemblage is represented by Ksp + Plg + Qtz + Ms + Bt. Kinematic indicators as the SC fabric and shear bands show consistent top-to-the-west oriented sense of movement (Fig. 8).

Fig. 8. Asymmetric SC fabric in porphyritic orthogneiss. This fabric originated during the D2 deformation and suggests top-to-the-west oriented sense of movement.



## Summary of Stop 1

The Měděnec synformal structure clearly shows that mafic eclogites appear at the base of the orthogneiss body. There is a clear jump in metamorphic conditions between mafic eclogites (25–26 kbar and 650–700 °C, Klápová et al. 1998, Yaxley and Klápová 1999) and basement metasediments (14.5 kbar and 600 °C – Konopásek 1998) on one side and between eclogites and orthogneisses (no PT data but stable plagioclase) on the other side. Thus, the presence of eclogites suggests a major tectonic boundary between the orthogneiss body and plagioclase schists, along which the eclogites appeared in the middle crust. This is major evidence that orthogneisses represent an allochthonous body which was thrust over the Saxothuringian sedi-

ments. This allochthonous body will be further described as the **Lower crystalline nappe**. PT conditions of the thrusting are recorded in plagioclase schists as well as garnetiferous micaschists. The thrusting was oriented to the west, as indicated by the  $L_2$  lineation and kinematic indicators in orthogneisses. This is consistent with structures observed in other parts of the Krušné hory Mts. (e.g., Mlčoch and Schulmann 1992).

Late  $F_2$  folding resulted in the development of kilometer-scale open folds (basins and domes) of synformal and antiformal shapes. This geometry seems to be determining further behavior of the nappe sequence during the D3 event.

## Stop 2

### D1 and D2 structures in eclogites – Meluzína

Jiří KONOPÁSEK, Karel SCHULMANN and Helena KLÁPOVÁ

The base of the Lower crystalline nappe is characterized by the presence of numerous bodies of mafic eclogites. Most of them are chemically comparable to tholeiitic oceanic basalts (MORB), some correspond to the high-alumina basalts or gabbros. Eclogite facies metamorphism was interpreted by Kláková et al. (1998) as a result of subduction of the Saxothuringian oceanic crust prior to continental collision.

#### Metamorphic conditions

Primary eclogite-facies mineral assemblage consists mainly of omphacite (30–50 vol.%, Jd content betw. 35–52 %) and garnet (15–50 vol.%); less abundant phases are amphiboles, white mica, quartz, zoisite and rutile. Eclogite facies metamorphic conditions of 650–700 °C at 25–26 kbar (Kláková et al. 1998) were estimated using the Grt–Cpx thermometer and the Grt–Cpx–Phe barometer.

#### Structures

Most of the eclogite-facies rocks in the central part of the Krušné hory Mts. show well-developed metamorphic foliation and strong mineral lineation. These structures are characterized by alternation of omphacite- and garnet-rich bands, as well as by preferred orientation of omphacites, and have developed during HP–MT metamorphic event. As the above described structures formed at PT conditions markedly different from those observed in surrounding rocks, these structures are attributed to the D1 stage of deformation (Fig. 9). The  $S_1$  foliation dips steeply S to SW, whereas the  $L_1$  lineation plunges consistently west at moderate to steep angles.

Brittle-ductile to brittle structures developed during the emplacement of the Lower crystalline nappe. They are represented mainly by asymmetrical intrafoliation boudinage, shear bands and brittle cracks. All these structures are filled by Qtz with Rt + Amp. Moreover, the emplacement of eclogites in the middle crust is associated with their hydration. This is indicat-

ed by numerous crystals of amphiboles poikilitically overgrowing Cpx + Grt foliation. These structures are ascribed to the D2 phase of deformation (Fig. 9).

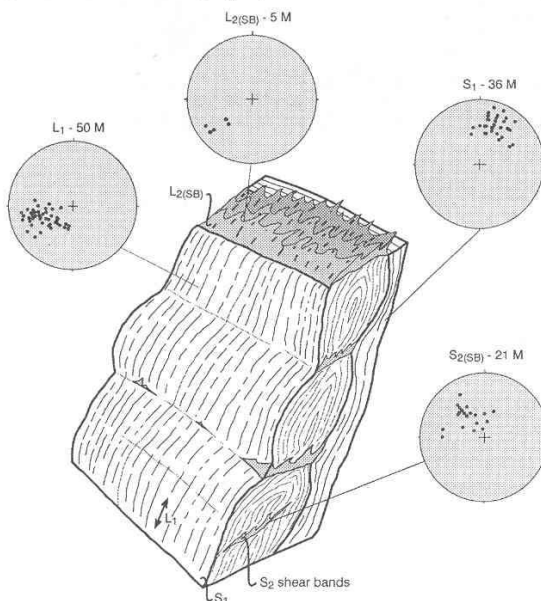


Fig. 9. A block diagram showing the D1 and D2 structures in eclogites, i.e. eclogitic foliation, asymmetrical foliation boudinage and oriented growth of minerals in neck zones. Orientation diagrams:  $L_1$  = mineral and stretching lineation;  $S_1$  = poles to eclogitic foliation;  $S_2(SB)$  = poles to shear bands;  $L_2(SB)$  = lineation on shear bands. Lower hemisphere equal-area projection (from Kláková et al. 1998).

## Summary of Stop 2

Mafic eclogites in the central part of the Krušné hory Mts. clearly show that structures characterized by preferred orientation of omphacites and by metamorphic layering have formed under different metamorphic conditions than early structures of surrounding acid rocks. This fully justifies their classification as the D1 structures.

Dating of this HP event was performed on eclogites from the German part of the Krušné hory Mts. by Schmädicke et al. (1995) and by von Quadt and Gebauer (1998). Schmädicke et al. (1995) obtained Sm–Nd (Grt–WR) ages of  $333 \pm 6$  and  $337 \pm 5$  Ma and Sm–Nd (Grt–Cpx–WR) age of  $360 \pm 7$  Ma. On the other hand, von Quadt and Gebauer (1998) were able to extract

zircon from some mafic eclogites and provided  $^{206}\text{Pb}/^{238}\text{U}$  mean SHRIMP age of  $490 \pm 14$  Ma for the protolith formation and conventional U–Pb single zircon age of  $342.5 \pm 1.6$  Ma reflecting the time of the HP metamorphism.

D2 structures, such as intrafoliation boudinage and shear bands, as well as the appearance of amphiboles are interpreted as the result of deformation under middle-crustal conditions. The peak pressure conditions of 14.5 kbar in surrounding metapelites correspond well to the fact that eclogitic assemblage was still stable during the initial stages of hydration as recorded by random growth of amphiboles within stable Grt–Cpx matrix.

## Stop 3 Refolding of a nappe sequence during the D3 deformation

Jiří KONOPÁSEK and Karel SCHULMANN

### Stop 3a

**Augen orthogneisses of the Klínovec antiform** represent the Lower crystalline nappe refolded during the D3 deformation. The  $S_{2,3}$  foliation is characterized by quartz and plagioclase ribbons. The E–W-trending, gently plunging lineation is characterized by stretching of mineral aggregates on the foliation plane (see Fig. 10 for orientation of the D3 structures). The  $S_{2,3}$  foliation strikes E–W and dips steeply S. This orientation suggests that the original D2 fabric is refolded by D3 compression-

al deformation resulting in steepening and rotation of the  $S_2$  foliation. Principal compression during the D3 phase was acting N–S as documented by the orientation of the  $S_{2,3}$  foliation in the Klínovec antiform. Numerous  $F_3$  folds with steep axial planes and subhorizontal axes in the basement metasediments support this interpretation.

The orientation of lineation is very important for the interpretation of the course of the D3 folding. Fig. 11 shows the

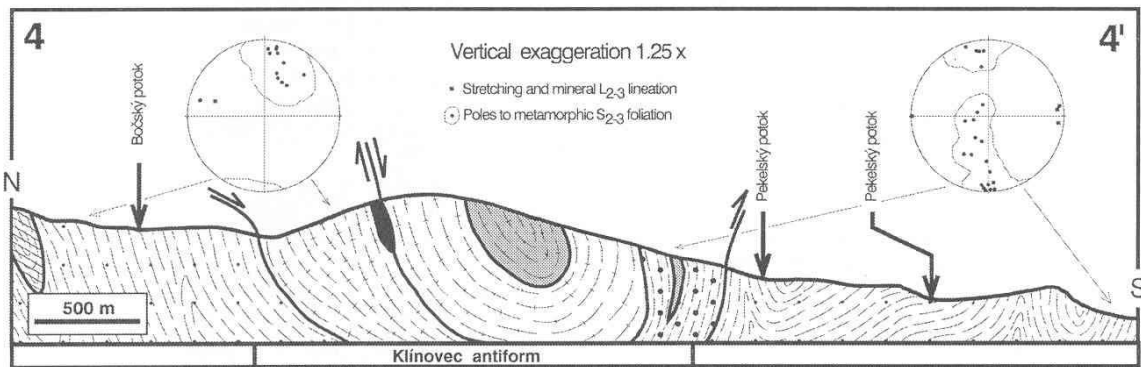


Fig. 10. Cross-section of the Klínovec antiform with D2-D3 structural data represented by the lower-hemisphere equal-area projection. Data are contoured at 1x uniform distribution. See Fig. 2 for the position of the cross-section and key to patterns of the rock types.

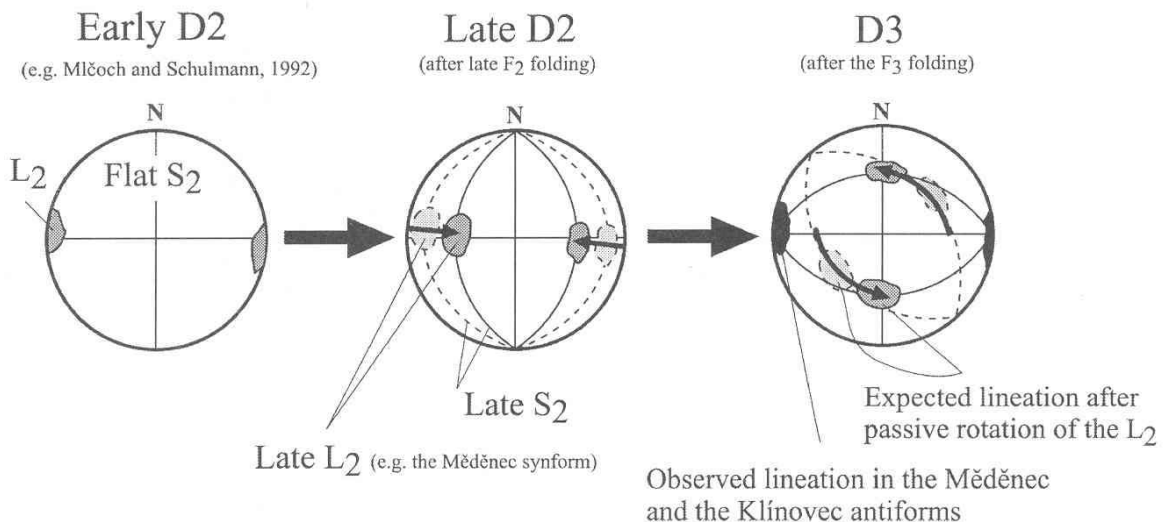


Fig. 11. Succession of the lower-hemisphere equal-area projections schematically illustrates the expected evolution of the orientation of  $L_2$  lineation during D2-D3. Early  $L_2$  lineation trends E–W and is subhorizontal. After late D2 deformation,  $L_2$  lineation does not change the orientation, but becomes steeper due to the development of large-scale, late  $F_2$  folds. The successive  $F_3$  folding changes the orientation of steep  $S_2$  foliation, and steep  $L_2$  lineation should rotate into N–S direction with steep plunge. However, in the D3 structures (Měděnec and Klínovec antiforms) the lineation always trends E–W and is mostly subhorizontal. This orientation suggests that in the D3 structures we are dealing with newly developed  $L_3$  lineation.

rotation of originally gently plunging, E–W trending  $L_2$  lineation. It demonstrates that passive rotation of early  $L_2$  lineation during late  $F_2$  folding and subsequent  $F_3$  folding will result in subvertical lineation. However, we consistently observe lineation trending E–W and gently plunging to the west in orthog-

neisses of the Klínovec antiform. Provided that our interpretation of the Klínovec antiform is correct, this observation suggests complete reworking of the  $L_2$  fabric during the D3 phase and thus E–W-oriented principal extension during the D3 phase.

### Stop 3b

**Plagioclase schists in the southern limb of the Klínovec antiform** show the same mineralogy as those from the Měděnec

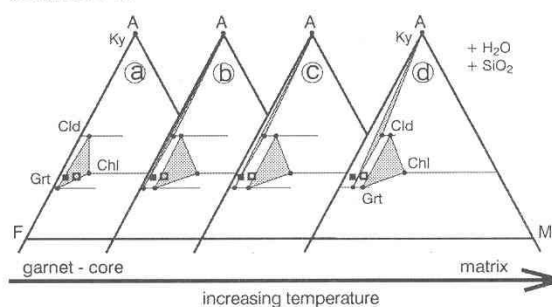
synform. The only difference is the presence of subvertical planar fabric herein interpreted as the  $S_3$  foliation.

### Stop 3c

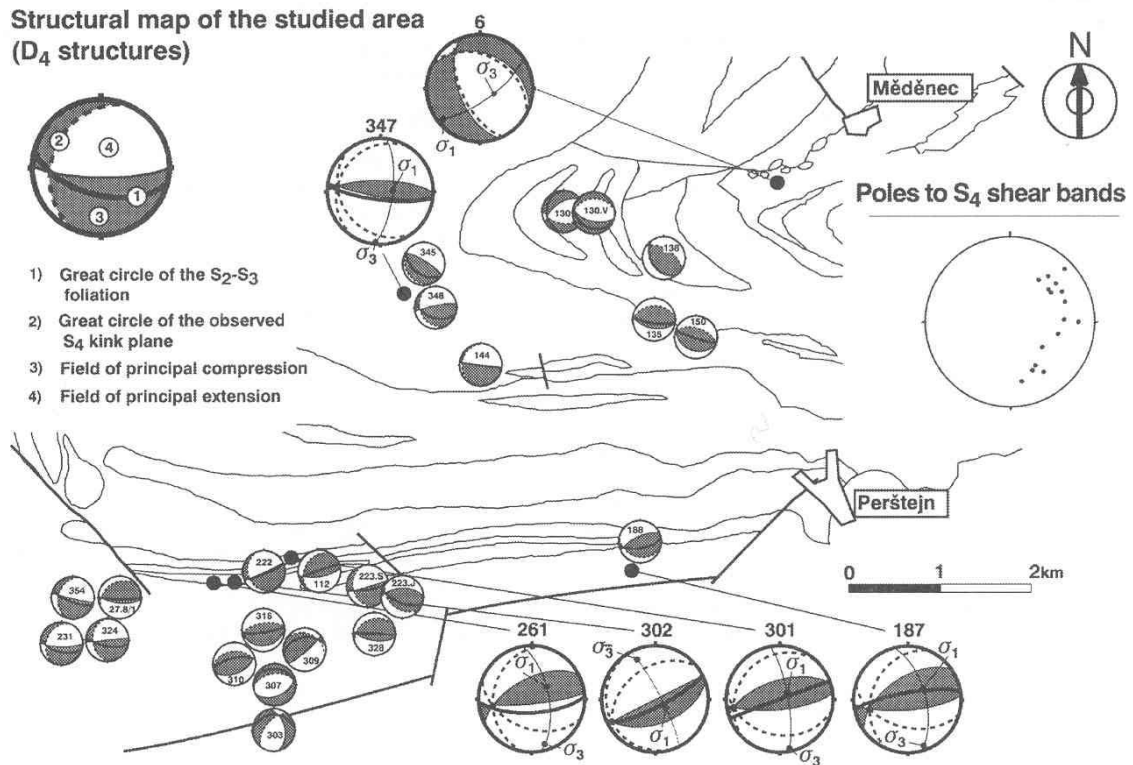
**Garnetiferous (Srní) micaschists** represent the basal sequence of the Lower crystalline nappe, as it is in the case in the Měděnec synform. However, mineral assemblages in samples from this locality differ from those in samples from locality 1b. Garnet porphyroblasts envelope mineral assemblage Cld + Chl I, whereas matrix consists of Cld + Chl II + Ms + Qtz. The difference in mineral assemblages between micaschists from this locality and locality 1b is attributed to the difference in the whole-rock composition (Fig. 12). As the micaschists from this locality contain more MgO, crystallization of kyanite is not possible and the two-phase assemblage Grt + Cld remains stable in the matrix. The appearance of Chl II is attributed to retrogression. Garnetiferous micaschists of the southern limb of the Klínovec antiform intercalate with a layer of amphibolites. These amphibolites contain mineral assemblage Grt + Pl + Amp ± Ep and show no evidence of eclogite-facies overprint.

At this locality, compressional  $F_4$  kink-band folds rework the subvertical  $S_3$  foliation (Fig. 13).  $F_4$  kink-band folds have subhorizontal axial planes and axes gently plunging to the west. These structures are ubiquitous in those parts of the study area

where steep foliation was produced by the D3 compression. In orthogneisses with subvertical foliation, the D4 occurs in the form of discrete shear planes crosscutting the metamorphic foliation at high angles. Two conjugate sets of the  $F_4$  kink-band folds were observed at many localities, allowing the determination of principal stresses during their formation. These structures suggest that the orientation of principal compression during the D4 phase was subvertical and principal extension was oriented N–S.



**Fig. 12.** Phase topology in the AFM system. The full black square corresponds to the assumed whole-rock composition of the Měděnec micaschists, the blank black square corresponds to the assumed whole-rock composition of the Srní micaschists. Internal triangles show changes in composition of the three-phase assemblages (garnet–chloritoid–chlorite and garnet–chloritoid–kyanite) observed between cores of garnet porphyroblasts and the matrix. a) Phase topology corresponding to the mineral assemblage observed in garnet cores in the Měděnec micaschists. The same continuous reaction (reaction (1)) is considered to be responsible for initial growth of garnet in the Srní micaschists. b) and c) Phase topologies corresponding to the assemblage of the intermediate zone of garnet porphyroblasts in the Měděnec micaschists, and the assemblage at rims of garnet porphyroblasts in the Srní micaschists (continuous reaction (1) is alternating with continuous reaction (2) in the Měděnec micaschists; in the Srní micaschists, garnet still grows by continuous reaction (1)). d) Phase topology observed in the matrix of both the Měděnec micaschists (all chloritoid consumed by reaction (2)) and of the Srní micaschists (all chlorite consumed by reaction (1)).



**Fig. 13.** Structural map of the study area showing D<sub>3</sub> and D<sub>4</sub> monoclinial and conjugate systems of kink bands. Orientation of the kink bands is presented in the lower-hemisphere equal-area projection together with the orientation of the S<sub>2</sub>-S<sub>3</sub> foliation (see upper left inset for principal fabric elements). For each locality (numbered in or above each projection), all measured kink bands and foliations were averaged and presented as a mean value. Estimated s<sub>1</sub> and s<sub>3</sub> directions are shown for localities with developed conjugate system of kink bands. The equal-area projection on the right of the figure represents poles to brittle-ductile, late D<sub>4</sub> shear bands in orthogneisses and micaschists.

### Summary of Stop 3

In the southern part of the study area, the thrust-related D<sub>2</sub> fabric is completely reworked by the D<sub>3</sub> deformation. Main compression changes from the E-W during the D<sub>2</sub> into the N-S during the D<sub>3</sub>. Large-scale F<sub>3</sub> folds developed (Klínovec and Měděnec antiforms) in response to the D<sub>3</sub> deformation. F<sub>3</sub> folding is associated with complete reworking of mineral lineation of orthogneisses suggesting E-W-oriented principal extension during the D<sub>3</sub> event.

Subsequent D<sub>4</sub> structures appear in rocks with subvertical S<sub>2-3</sub> foliation and are consistent with vertical orientation of the principal compression. This change in the principal stress orientation is interpreted as a result of disappearance of horizontal D<sub>3</sub> compression and increasing role of the overburden during uplift of the whole thickened rock sequence.

## Stop 4

### Kadaň dam – the Upper crystalline nappe

Simona KRÁLÍČKOVÁ, Jiří KONOPÁSEK and Karel SCHULMANN

A metamorphic unit exposed in the Ohře River valley in the footwall of the Tertiary volcanites is composed mainly of HT orthogneisses, granulites and granulitic gneisses. In the present interpretation of large-scale units of the Bohemian Massif, this so-called Eger crystalline unit represents the easternmost part of the Saxothuringian domain. Kotková (1993) studied metamorphic conditions of granulites and the PT estimates for the peak-pressure stage are in the range of 700–800 °C at 15–18 kbar. Metamorphic age of  $342 \pm 5$  Ma for this HP event was derived from metamorphic zircons by Kotková et al. (1996).

Mineral assemblage of the HT orthogneisses is  $Ksp + Plg + Qtz + Bt + Grt \pm Ms \pm Ky$ . Muscovite-free, kyanite-bearing orthogneisses show the same mineralogy as acid granulites exposed in this unit. Microstructural characteristics of the orthogneiss change even at the scale of the outcrop suggesting an important role of deformation and water availability during metamorphic processes.

A similar unit appears in the German part of the central Krušné hory Mts. (Zöblitz granulites and granulitic gneisses). Here, Willner et al. (1997) studied metamorphic evolution of granulitic rocks and their PT estimates (830 °C at 21 kbar) roughly agree with those derived by Kotková (1993) from the Eger granulites. Moreover,  $^{207}Pb/^{206}Pb$  zircon ages of 341–342 ± 0.5 Ma from these granulites correspond with those derived by Kotková et al. (1996) from the Eger granulites. We therefore suggest

that HT orthogneisses intercalated with acid granulites represent another nappe body thrust over both the basement metasediments and the Lower crystalline nappe. Consequently, the Eger crystalline unit will be further termed the *Upper crystalline nappe*.

#### Microstructural evolution

Four stages of metamorphic evolution of HT orthogneisses can be distinguished at this locality: 1) coarse-grained augen orthogneiss, 2) banded anatectic orthogneiss, 3) fine-grained migmatitic gneiss and 4) granulitic gneiss.

Coarse-grained augen orthogneiss is composed of monomineralic polycrystalline layers of equigranular Plg and Kfs grains meeting at triple points, and mica-bearing domains separating these layers from less deformed quartz lenses. Subsequent stage of microstructural evolution is characterized by lining of K-feldspar boundaries by quartz. Quartz films grow and, together with plagioclase, progressively destroy monomineralic K-feldspar aggregates. The resulting texture is characterized by polymineralline aggregates separated by discontinuous domains of mica and abundant crystals of garnet. Last stage is characterized by completely recrystallized fine-grained omnidirectional granulitic structure with abundant garnet porphyroblasts. Lower amount of biotite relative to other rock types is typical for this stage.

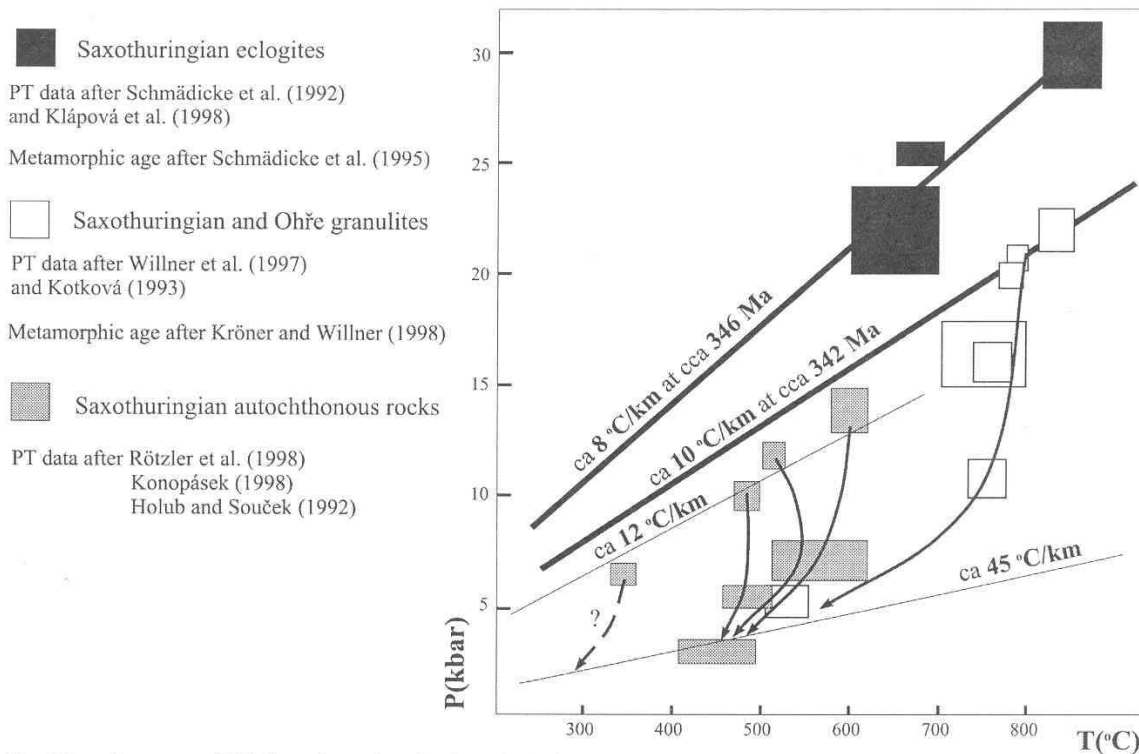


Fig. 14. Summary of PT data shows that the Saxothuringian eclogites and granulites of the Upper crystalline nappe have formed at the same time, but under contrasting thermal gradients.

## Structures

In our interpretation, the main metamorphic foliation is termed  $S_3$ . The reason for this is its subvertical orientation and E–W strike, which is consistent with the  $S_3$  foliation in the basement and the Lower crystalline nappe. The  $S_3$  foliation is characterized by ribbons of completely recrystallized K-feldspar, plagioclase and quartz. However, the feldspar ribbons are not monomineralic – the reason is explained in the section on microstructures. The  $L_3$  lineation does not show uniform orientation suggesting extreme ductility of the rock during the D3 deformation.

The D3 fabric is further refolded by the D4 deformation. The D4 deformation produced  $F_4$  folds with flat or westerly dipping axial planes and axes gently plunging to the west. The orientation of the  $F_4$  folds suggests vertical shortening which is in accord with the orientation of principal stresses during the D4 in the basement metasediments and orthogneisses of the Lower crystalline nappe.

## Conclusions

The excursion has demonstrated that there are two crystalline nappes overlying the Saxothuringian metasedimentary basement. The D1 structures are present exclusively in eclogites and cannot be correlated with early structures in the surrounding rocks. The D2 structures are associated with westward thrusting of allochthonous units and represented by main metamorphic foliation in all non-eclogitic lithologies. The geometry of the D3 structures suggests significant compressional event with principal compression acting in N–S direction. Final brittle-ductile D4 structures suggest an increasing role of the overburden during late stages of exhumation. The D1–D3 structures in the study area are compressional and exclude significant contribution of ductile extension to exhumation of the Saxothuringian middle crust.

A question arises whether both crystalline nappes belong to the Saxothuringian domain as it is generally accepted. Acid granulites and eclogites yielded the same zircon metamorphic age of 342 Ma. However, these rocks formed under completely different thermal conditions (Fig. 14). This observation suggests that whereas eclogites are interpreted as subducted Saxothuringian oceanic crust, granulites and orthogneisses of the Upper crystalline nappe formed in a domain with higher thermal gradient. PT conditions of the Lower crystalline nappe are not known, but the presence of eclogites at its base suggests that they cannot be derived from the Saxothuringian domain as the so-called “basement-derived nappe”. Therefore, we are of the opinion that the eastern boundary of the Saxothuringian domain in the central part of the Krušné hory Mts. lies between the basement plagioclase schists and the Lower crystalline nappe.

## References

- HOTH K., WASTERNAK J., BERGER H.-J., BREITER K., MLČOCH B. and SCHOVÁNEK P., 1994. Geologische Karte Erzgebirge/Vogtland – 1:100 000. Sächsisches Landesamt für Umwelt und Geologie.
- KLÁPOVÁ H., KONOPÁSEK J. and SCHULMANN K., 1998. Eclogites from the Czech part of the Erzgebirge: multi-stage metamorphic and structural evolution. *J. Geol. Soc., London*, 155: 567–583.
- KONOPÁSEK J., 1998. Formation and destabilization of the high pressure assemblage garnet-phengite-paragonite (Krušné hory Mountains, Bohemian Massif): The significance of the Tschermak substitution in the metamorphism of pelitic rocks. *Lithos*, 42: 269–284.
- KONOPÁSEK J. High-pressure garnetiferous micaschists in the central part of the Krušné hory Mountains (Bohemian Massif). *Eur. J. Mineral.*, (in print).
- KOTKOVÁ J., 1993. Tectonometamorphic history of lower crust in the Bohemian Massif – example of north Bohemian granulites. *Czech Geol. Surv. Spec. Pap.*, 2: 56 pp.
- KOTKOVÁ J., KRÖNER A., TODT W. and FIALA J., 1996. Zircon dating of North Bohemian granulites, Czech Republic: further evidence for the Lower Carboniferous high-pressure event in the Bohemian Massif. *Geol. Rundsch.*, 85: 154–161.
- KROHE A., 1996. Variscan tectonics of Central Europe: post-accretionary intraplate deformation of weak continental lithosphere. *Tectonics*, 15: 1364–1388.
- KRÖNER A. and WILLNER A.P., 1998. Time of formation and peak of Variscan HP-HT metamorphism of quartz-feldspar rocks in the central Erzgebirge, Saxony, Germany. *Contrib. Mineral. Petrol.*, 132, 1: 1–20.
- MLČOCH B. and SCHULMANN K., 1992. Superposition of Variscan ductile shear deformation on pre-Variscan mantled gneiss structure (Catherine dome, Erzgebirge, Bohemian Massif). *Geol. Rundsch.* 81 (2): 501–513.
- VON QUADT A. and GEBAUER D., 1998. Evolution of eclogitic rocks in the Erzgebirge: A conventional and SHRIMP U-Pb zircon and Sm-Nd study. *Acta Univ. Carolinae Geologica*, 42, 2: 324–325.
- RÖTZLER K., SCHUMACHER R., MARESCH W.V. and WILLNER A.P., 1998. Characterization and geodynamic implications of contrasting metamorphic evolution in juxtaposed high-pressure units of the Western Erzgebirge (Saxony, Germany). *Eur. J. Mineral.*, 10: 261–280.
- SATTRAN V., 1967. Geological map of the central part of the Krušné hory Mountains between Klášterec nad Ohří and Vejprty in the Czech Republic. *Unpublished*.
- SCHMÄDICKE E., OKRUSCH M. and SCHMIDT W., 1992. Eclogite-facies rocks in the Saxonian Erzgebirge, Germany: high pressure metamorphism under contrasting P-T conditions. *Contrib. Mineral. Petrol.*, 110: 226–241.
- WILLNER A.P., RÖTZLER K., KROHE A., MARESCH W. and SCHUMACHER R., 1994. Druck-Temperatur-Deformations-Entwicklung verschiedener Krustengesteine im Erzgebirge: Eine Modellregion für die Exhumierung von Krustengesteinen. *Terra Nostra*, 3/94: 104–106.
- WILLNER A.P., RÖTZLER K. and MARESCH W.V., 1997. Pressure-Temperature and fluid evolution of quartzo-feldspathic metamorphic rocks with a relic high-pressure, granulite-facies history from the Central Erzgebirge (Saxony, Germany). *J. Petrol.* 38: 307–336.
- YAXLEY G.M. and KLÁPOVÁ H., 1999. The metamorphic evolution of carbonate-bearing eclogites from the Saxothuringian zone (Czech Republic). *Krystalinikum*, 25: 143–161.